INVESTIGATING THE EFFECTS OF *MYO*-INOSITOL PHOSPHATES ON HUMAN CANCER CELLS

DAVID WITTEN
Bachelor of Science, **University of Lethbridge**, **2021**

A thesis submitted
in partial fulfilment of the requirements for the degree of

MASTER OF SCIENCE

in

BIOCHEMISTRY

Department of Chemistry and Biochemistry
University of Lethbridge
LETHBRIDGE, ALBERTA, CANADA

INVESTIGATING THE EFFECTS OF *MYO*-INOSITOL PHOSPHATES ON HUMAN CANCER CELLS

DAVID WITTEN

Date of Defence: July 30th, 2024

Dr. Roy Golsteyn	Professor	Ph.D.
Dr. Steven Mosimann	Associate Professor	Ph.D.
Thesis Co-Supervisors		
Dr. Elizabeth Schultz	Professor	Ph.D.
Thesis Examination Committee Member		
Dr. Nehal Thakor	Professor	Ph.D.
Thesis Examination Committee Member		
Dr. Dylan Girodat	Assistant Professor	Ph.D.
Chair, Thesis Examination Committee		

ABSTRACT

In this thesis we investigate the effects of *myo*-inositol phosphates on human cancer cells. We determined that $InsP_6$ and two $InsP_5$ isomers, specifically $Ins(2,3,4,5,6)P_5$ and $Ins(1,2,4,5,6)P_5$, induce vesicle formation in the ER of two human cancer cell lines. We also determined that $Ins(1,2,3,4)P_4$ did not induce vesicles in cells. We predict that the specificity of the vesicle phenotype is limited to higher-phosphorylated IPs. This is the first time either $InsP_5$ isomer has been exogenously applied to cells in vitro. To our knowledge, we are also the first to report IP-mediated vesicle formation within the ER in any human cell line. Additionally, $InsP_6$, $Ins(1,2,4,5,6)P_5$ and $Ins(2,3,4,5,6)P_5$ formed precipitate in cell culture media whereas $Ins(1,2,3,4)P_4$ did not. Occurrence of IP precipitation in cell culture media is noted in the literature, yet little is known about the effect the precipitate has on cells itself. Despite observing that IP precipitation occurred simultaneously with the vesicle phenotype, we determined that the precipitate itself was not cause of vesicle formation. We also determined that vesicle formation was not due to extracellular cation depletion by the precipitate as EGTA and DFO could not induce a similar effect. The effects of $InsP_6$ are relatively well characterized in vitro, yet its mechanism of action often remains ambiguous. Therefore, the novel discovery that $InsP_6$ and two chemically related $InsP_5$ isomers induce vesicle formation in the ER of human cancer cells offers new insights relevant to mechanistic discussion behind exogenous $InsP_6$ effects, especially those already present in the literature.

ACKNOWLEDGEMENTS

I would like to offer my deep gratitude to my supervisors Dr. Roy Golsteyn and Dr. Steve Mosimann for their supervision over the last years. Besides their excellent academic mentorship, their genuine friendship has left a deep impact on my life. I have been privileged to learn from them not only as senior scientists, but also as friends.

I would like to thank my committee members Dr. Nehal Thakor and Dr. Elizabeth Shultz for their support and discussions throughout my graduate studies. Thank you to Dr. Dylan Girodat for acting as chair of my committee.

Thank you to the past and present members of the Natural Product Lab Tanner Lockwood, Larissa Smith, Shannon Healy Knibb, Brinnley Zanewich, Haley Allard, Araba Sagoe-Wagner, and Nadia Hand; I have enjoyed the friendship and support that came from working with you all. I would like to specifically thank Colyn Cleland in Dr. Mosimann's Lab for his early mentorship in my scientific career and his continued friendship. The friendship of Josh Craig, Jinay Patel, Dr. Vineet Rathod, and Catherine McCord has also meant much to me throughout my graduate studies.

Finally, thank you to my parents, and my sister Laura; they have always listened to my thoughts and spurred me on to excellence.

TABLE OF CONTENTS

LIST OF TABLES

LIST OF FIGURES

LIST OF ABBREVIATIONS

ANOVA	one-way analysis of variance
ATCC	American Type Culture Collection
ATP	adenosine triphosphate
CsA	cyclosporine A
DFO	deferoxamine
DMEM	Dulbecco's Modified Eagle Medium
DMSO	dimethyl sulfoxide
DNA	deoxyribonucleic acid
ECM	extracellular matrix
EDTA	ethylenediaminetetraacetic acid
EGTA	ethylene glycol bis-(2-aminoethylether)-N,N,N',N'-tetraacetic acid
ER	endoplasmic reticulum
FBS	fetal bovine serum
h	hours
HEPES	4-(2-hydroxyethyl)-1-piperazineethanesulfonic acid
HT-29	Human colorectal adenocarcinoma cell line
ICP-MS	inductively coupled plasma mass spectroscopy
$InsP_6$	*myo*-inositol-1,2,3,4,5,6-hexakisphosphate
$Ins(1,2,4,5,6)P_5$	*myo*-inositol-1,2,4,5,6-pentakisphosphate
$Ins(2,3,4,5,6)P_5$	*myo*-inositol-2,3,4,5,6-pentakisphosphate
$Ins(1,3,4,5,6)P_5$	*myo*-inositol-1,3,4,5,6-pentakisphosphate
$Ins(1,2,3,4)P_4$	*myo*-inositol-1,2,3,4-tetrakisphosphate
$Ins(1,2,3)P_3$	*myo*-inositol-1,2,3-trikisphosphate
$Ins(1,4,5)P_3$	*myo*-insoitol-1,4,5-trikisphosphate
Ins	*myo*-inositol
IP	*myo*-inositol phosphate
IUPAC	International Union of Pure and Applied Chemistry
MDD-HPIC	metal-dye detection high performance ion chromatography
MEM-NEAA	Modified Eagle Medium non-essential amino acids
NR	Nile Red
PBS	phosphate buffered saline
PPT	precipitate
SEM	standard error of the mean
U2-OS	Human osteosarcoma cell line

CHAPTER 1

Introduction

This thesis is about the biological effects of *myo*-inositol phosphates (IPs) on human cancer cells. A wide range of biological effects have been attributed to IPs. This research has been limited by the source of IPs as they are difficult to chemically synthesize or purify from natural sources. As a result, the potential biological function of many IPs has not been studied. In the present project, previous work in Dr. Mosimann's laboratory provided unique access to IPs not commercially available and not reported in eucaryotic cells . We analyzed *myo*-inositol hexa*kis*phohspahte ($InsP_6$), a common IP, as well as three unique, enzymatically derived IPs from our own research program. We found that $InsP_6$ and two of our unique IPs induced vesicle formation in the endoplasmic reticulum (ER) of human cancer cells. Despite $InsP_6$ being relatively well characterized in vitro, we are the first to report vesicle formation in human cancer cells upon $InsP_6$ treatment. We were also able to determine that the effect is not specific to $InsP_6$ given that two related IPs induce the same vesicle phenotype. To discuss the observed effect of vesicle formation in cells upon treatment with IPs, we will introduce the chemical structure of IPs, their known biological effects, and several challenges facing in vitro IP research.

1.1 *Myo*-inositol phosphates

Myo-inositol phosphates (IPs) are a diverse group of chemically distinct but related compounds. They are ubiquitous in eucaryotic cells and play key roles in cellular processes. Their structural complexity facilities their diverse functions yet this complexity introduces challenges when considering IP research. To understand better these challenges, we will provide a detailed discussion of their structure.

1.1.1 Chemical structure of *myo*-inositol

Inositols are a family of 6 carbon, cyclic carbohydrates with hydroxyls at each carbon (Figure 1.1). The inositol family is made up of 9 stereoisomers of cyclohexanehexol, of which *myo*-inositol is the most abundant in biological systems (Michell, 2008b; Murthy, 2006). *Myo*-inositol is most energetically stable in its chair conformation with the 1 hydroxyl in the axial position and the other 5 hydroxyls in the equatorial position (Michell, 2008a). *Myo*-inositol is a meso-compound with a plane of symmetry through the C2 and C5 carbons and is therefore achiral despite having chiral centers. Splitting the molecule along the plane of symmetry results in two non-superimposable, mirror images with the remaining carbons forming prochiral pairs at C1/C3 and C4/C6 (Loewus & Murthy, 2000). Numbering of the carbons within each prochiral pair can be conducted according to the D- or L- configuration. IUPAC recommendations specify the D- numbering system be used by default (Figure 1.1). Thus, the abbreviated prefix, Ins, represents *myo*-inositol in the D- configuration (Murthy, 2006).

1.1.2 Chemical structure of *myo*-inositol phosphates

Each hydroxyl in *myo*-inositol can form a phosphodiester bond with a phosphate, resulting in 63 unique phosphorylated derivatives of *myo*-inositol, termed *myo*-inositol phosphates (IPs). Of these 63 theoretical IPs, *myo*-inositol-1,2,3,4,5,6-hexakisphosphate ($InsP_6$ or phytic acid) is the most abundant in nature (Irvine & Schell, 2001). In solution, $InsP_6$ adopts the energetically favourable 1-axial/5-equatorial chair conformation for pH values <9.2. Between pH 9.2 and 9.6, $InsP_6$ exists in a dynamic equilibrium between the sterically favored 1-axial/5-equatorial conformation and sterically unfavourable 5-axial/1-equatorial conformation. Above pH 9.6, $InsP_6$ primarily exists in the 5-axial/1-equatorial

conformation (Isbrandt & Oertel, 1980). These values were determined in vitro and strongly depend on other factors such as ionic strength and presence of multi-valent cations.

Each phosphoryl can be protonated twice resulting in 12 total protonation sites on $InsP_6$ (Figure 1.1). The first six sites – one on each of the six phosphoryl groups - are strongly acidic with pKa values between 1.1 and 2.1. The next three sites have pKa values in the physiological range of 6.0-7.6, whereas the last three sites correspond to the total deprotonation (and subsequent conformation inversion) of $InsP_6$ with pKa values between 9.2 and 9.6 (Costello et al., 1976). As a result, $InsP_6$ carries a highly negative overall charge in physiological systems (usually between -6 and -9). Importantly, these physiochemical properties differ as a function of phosphorylation of the *myo*-inositol backbone, since the presence or absence of one phosphoryl group changes the microenvironment of the remaining phosphoryl groups (Barrientos & Murthy, 1996).

Like *myo*-inositol, $InsP_6$ is an achiral mesocompound. Drawing a plane of symmetry through the C2 and C5 carbons of $InsP_6$ results in two non-superimposable, mirror images. Dephosphorylation of specific phosphoryl groups may render the IP chiral by removing the plane of symmetry. For example, Ins(2,3,4,5,6)P_5 is a chiral molecule due to the absent C1 phosphoryl. Ins(2,3,4,5,6)P_5 is an enantiomer of Ins(1,2,4,5,6)P_5 as they differ at phosphorylation states within the enantiotopic C1/C3 pair. These two enantiomers are chemically equivalent and will interact with achiral molecules such as divalent cations without specificity whereas a chiral reagent such as an enzyme will select between them preferentially. This phenomenon extends to all IPs that differ in phosphorylation state between the C1/C3 and/or C4/C6 prochiral pairs alone.

1.1.3 Limited availability of *myo*-inositol phosphates

Of the 63 theoretical IPs, approximately half have been reported in nature. Of the IPs reported, many have critical cellular roles. As a result, the elucidation of biological functions of all IPs has acquired significant attention (Best et al., 2010). A limiting factor in this search is the unavailability of most IPs. IPs are obtained either by extraction from natural sources or chemical synthesis. Some IPs such as $InsP_6$ are present at high concentrations in natural sources like plant seeds and are thus readily available for research. However, most lower phosphorylated IPs have no significant natural source, limiting their access to chemical synthesis (Potter & Lampe, 1995). Specifically, all IPs, excluding $InsP_6$, sourced from natural sources, lack the C2 phosphoryl. Consequently, the biological roles of common IPs such as $InsP_6$ have become relatively well characterized while those of the less available IPs remain ambiguous. Because of previous research in Dr. Mosimann's laboratory, we have unique access to enzymatically derived IPs, all of which contain the C2 phosphoryl (Bruder et al., 2017). This access presents an opportunity to study their potential biological functions. This is a central significance of our research.

1.2 Biological roles of *myo*-inositol phosphates

1.2.1 $InsP_6$

$InsP_6$ was first discovered in 1855 by Theodor Hartig while studying small circular particles in plant seeds (Hartig, 1855). Later, these particles were found to be a source of phosphorus, calcium and magnesium. The substance in these particles was termed "phytin" on account of its botanical origin, having not been observed in other biological sources like meat or dairy. In 1897, the presence of *myo*-inositol in phytin was discovered by its reaction

with hydrochloric acid, which released phosphoric acid and *myo*-inositol. This discovery paved the way for the elucidation of $InsP_6$'s structure in 1914.

The initial understanding of $InsP_6$ as a storage molecule has evolved to include a host of biological roles. Historically, $InsP_6$ has been considered a signaling molecule. More recently it has been acknowledged that $InsP_6$ does not fit the classical understanding of a signaling molecule as no evidence suggests it undergoes stimulus-dependent changes in intracellular concentration (Shears et al., 2012). Rather, $InsP_6$ is now understood to be a key co-factor in cellular processes. For example, $InsP_6$ is a co-factor in processes such as mRNA export, DNA repair, bacterial pathogenicity, plant hormone receptor regulation, apoptosis, and vesicle trafficking (Anderson & Wolter, 1966; Hanakahi et al., 2000; Macbeth et al., 2005; Majerus et al., 2008; Potter & Lampe, 1995; Smith et al., 1994; Tan et al., 2007; York et al., 1999). This list is not comprehensive, but it provides a sample of the diverse yet universal functions of $InsP_6$.

$InsP_6$ has also received much attention in health and nutrition. There is growing evidence that $InsP_6$ has therapeutic potential for conditions such as diabetes, osteoporosis, neurodegenerative diseases, pathogenic calcifications, and various cancers (Dilworth et al., 2023; Pujol et al., 2023; Shamsuddin et al., 1997). $InsP_6$ is the subject of several ongoing clinical trials reviewed by Pires and colleagues regarding these conditions (Pires et al., 2023). Additionally, $InsP_6$ contains well characterized antioxidant and anti-inflammatory activity (Urbano et al., 2000). As a result, several studies have focused on the benefit of dietary $InsP_6$ in nutrition (Pujol et al., 2023). Conversely, $InsP_6$ has negative effects such as reduced absorption of essential minerals in humans and animals (Schlemmer et al., 2009). The reduced bioavailability of cations such as iron, zinc and calcium can disrupt

homeostasis in humans with serious health effects. In the case of animals, the agriculture industry utilizes enzymes known as phytases that can be included in animal feed. These phytases increase mineral availability and animal growth by dephosphorylating $InsP_6$, thereby liberating any chelated cations. The inclusion of these phytases in animal feed is commonplace and made up an industry valued above 550 million USD in 2023. Taken together, the diverse range of effects and broad implications of $InsP_6$ make it a significant bioactive molecule.

1.2.2 Other *myo*-inositol phosphates

Like $InsP_6$, *myo*-inositol penta*kis*phosphate ($InsP_5$) functions as a cofactor for eucaryotic enzymes. Although 6 theoretical isomers of $InsP_5$ exist, only specific isomers have biological roles. Of these, Ins(1,3,4,5,6)P_5 appears to be the most abundant in eucaryotic cells and is a key metabolic link between the less-phosphorylated IPs ($InsP_4$ and $InsP_3$) and $InsP_6$ (Irvine & Schell, 2001). The characterized biological roles of Ins(1,3,4,5,6)P_5 include regulation of oxygen binding to hemoglobin, viral assembly, chromatin remodeling, regulation of L-type Ca^{2+} channels, and cytoskeletal reorganization (Borgese & Nagel, 1977; Campbell et al., 2001; Heslop et al., 1985; Komander et al., 2004; Quignard et al., 2003; Steger et al., 2003). Ins(1,3,4,5,6)P_5 has also been shown to promote apoptosis by competitively inhibiting the binding of phosphatidylinositol-3,4,5-triphosphate (PtdIns(3,4,5)P_3) to the pleckstrin homology (PH) domain of Akt/PKB, thereby preventing the protein's localization to the membrane (Piccolo et al., 2004). While other water-soluble IPs have been implicated in the competitive inhibition of cytosolic PH domains, Ins(1,3,4,5,6)P_5 is most notable. The biological roles of the remaining $InsP_5$ isomers, specifically those with the C2 phosphoryl, are not known.

The less-phosphorylated IPs, $InsP_4$ and $InsP_3$, are the most numerous and diverse class of IPs. Unlike the higher-phosphorylated IPs, $InsP_4$ and $InsP_3$ are considered classical 2nd messengers that regulate key biological transduction cascades. Briefly, these less-phosphorylated IPs have been implicated in biological roles such as chloride channel regulation, hormone signaling, chromatin remodeling, gene expression, and calcium mobilization from the ER (Odom et al., 2000; Shen et al., 2003; Steger et al., 2003; Vajanaphanich et al., 1994). The last of these is by far the most well-known and well-characterized function of any *myo*-inositol phosphate to date. Calcium release by the ER is regulated by direct binding of $Ins(1,4,5)P_3$ to $InsP_3$ receptors on the ER membrane (Berridge & Irvine, 1989). Interestingly, the interlinked and rapid metabolism of less-phosphorylated IPs has been shown to create a pool of accessory IPs (specifically $Ins(1,3,4,5)P_4$) capable of priming cells for, and thereby altering, the effect of $Ins(1,4,5)P_3$ signaling (Irvine & Schell, 2001).

Many other IPs with known functions, as well as several classes of molecules such as the pyrophosphates and phosphoinositides which are closely linked and interconverted with IPs, are not discussed here but are reviewed by Maffucci and colleagues (Maffucci & Falasca, 2020).

1.3 In vitro assays on *myo*-inositol phospahtes

The basis of IPs' potential as therapeutic agents comes from assays in vitro. Due to its availability, $InsP_6$ has been studied the most. For example, the antioxidant, anti-inflammatory and anti-cancer properties of $InsP_6$, have all come in part from experiments in vitro in which $InsP_6$ has been exogenously applied to human cell lines. Less is known about the other IPs as very few groups have access to these IPs, despite their potential

bioactivity. Here we recognized a knowledge gap, in that we had the opportunity to observe the effects of IPs not yet tested on human cell lines.

However, exogenously applying IPs in cell culture models has several challenges. These are due in part to the complexity of IPs. Unlike most natural products, the physiochemical properties of IPs make them particularly difficult to research in vitro. In some cases, this has led to the legitimacy of specific IP effects, most notably $InsP_6$'s anti-cancer activity, to be criticized in the literature on the basis that the interpretations of their supporting experiments are overly reductionistic. Our research, though unique, was not free of these complexities and the confounding variables they present. Therefore, we will introduce the main challenges of IP research in vitro, and the controversies surrounding certain claimed effects of IPs.

1.4.1 Cation chelation by higher *myo*-inositol phosphates

The high negative charge density of IPs, especially the higher-phosphorylated IPs, makes them potent cation chelators, especially multivalent cations (Luttrell, 1994). For example, at physiological pH, $InsP_6$ carries a net charge between -6 and -9 making it unique even among other polyanions. Consequently, $InsP_6$ can chelate various divalent cations with greater affinity than popular chelators like ethylenediaminetetraacetic acid (EDTA) and ethylene glycol bis-(2-aminoethylether)-N,N,N',N'-tetraacetic acid (EGTA) (Bohn et al., 2008). $InsP_5$ isomers share similar charge density and corresponding chelating potential (Hawkins et al., 1993). However, a change is observed in the lower phosphorylated IPs such as $InsP_4$ and $InsP_3$. These lower IPs have relatively weaker cation affinity (Lonnerdal et al., 1989; Luttrell, 1993), setting up a spectrum where the structure (number of phosphoryls) is an indicator of function (cation binding affinity). Stereospecificity of

phosphoryl locations on the *myo*-inositol backbone leads to exceptions to this spectrum. For example, whereas most $InsP_3$ isomers lack cation affinity, Ins(1,2,3)P_3 binds ferrous iron tightly (Minihane & Rimbach, 2002). This is because the 1,2,3 – phosphoryl motif has been shown to be pivotal in chelating Fe^{3+}. However, in general, $InsP_6$ and $InsP_5$ bind multivalent cations tighter than $InsP_4$ and $InsP_3$ (Skoglund et al., 1998).

Many biological functions of IPs are based on their chelating properties. These functions are not due to direct interactions of IPs with protein targets but are indirect effects due to altered cation pools. For example, the antioxidant activity of $InsP_6$ is largely due to its chelation of free iron, thereby protecting against oxidative damage (Minihane & Rimbach, 2002). $InsP_6$ has also been shown to prevent the formation of kidney stones in rats through calcium chelation (Grases et al., 1998). Distinguishing between direct effects of an IP and indirect effects via cation chelation can often be difficult. In 1987 an article in Nature inaccurately claimed both $InsP_6$ and $InsP_5$ were neurotransmitters in the mammalian brain (Vallejo et al., 1987). The article proposed that these two IPs may function as signaling molecules, similar to Ins(1,4,5)P_3. It was later shown that these higher IPs were not neurotransmitters but that they influenced neurotransmission by chelating neuronal calcium pools (Sun et al., 1992). Therefore, as Shears pointed out, careful attention should be given to assessing the functional specificity of any IP (Shears, 2001).

The challenge of cation chelation adds specific difficulty to in vitro assays. All cell culture models require divalent metal cations for cell growth and survival (Weiskirchen et al., 2023). While specific cell culture media compositions can vary, most media contain concentrations of calcium and magnesium in the micro to millimolar range with other essential metals present at lower, trace concentrations. When $InsP_6$ is added to these media,

it is likely that their divalent cation pools are affected by IP chelation. This argument forms the basis of the controversy surrounding $InsP_6$ as an anti-cancer agent.

For the last 3 decades multiple studies have noted the antiproliferative effect of $InsP_6$ on human cancer cells in vitro (Bizzarri et al., 2016; Rizvi et al., 2006; Shamsuddin et al., 1997; Vucenik, 2019). The effects appear broad, occurring in dozens of diverse cell lines (Brehm & Windhorst, 2019). Yet the mechanism by which $InsP_6$ exerts its antiproliferative effect is controversial. Some researchers have attributed it to direct interactions of $InsP_6$ with specific protein targets in the Akt pathway (Liu et al., 2015). Others hypothesize that the dephosphorylated products of $InsP_6$ account for its observed antiproliferative effect (Fu et al., 2016). However, Shears and Irvine dismiss both hypotheses on the basis that cation depletion is a more obvious explanation (Letcher et al., 2008; Shears, 2001). While the number of studies showing reduced cell progression in vitro is in the dozens, nearly all reports only saw the effect at high concentrations of 500 μM to 5 mM $InsP_6$. At these concentrations of $InsP_6$, Letcher argues, it can be assumed that cation depletion alone would induce an antiproliferative effect.

1.4.2 Precipitation with cell culture media components

Another characteristic of IPs, especially the higher IPs, is their tendency to form insoluble precipitates with cations in solution (Bohn et al., 2008; Torres et al., 2005; Veiga et al., 2006). In the context of experiments in vitro using $InsP_6$, this precipitation is a concern. Most cell culture media contain sufficient divalent cations to precipitate micromolar concentrations of $InsP_6$ as insoluble complexes (Letcher et al., 2008). Given the standard conditions of in vitro experiments using $InsP_6$ it could be assumed that the precipitate phenomenon is likely present in these experiments (Shears, 2001). However

few groups acknowledge this complexity in their reports. Encountering $InsP_6$ precipitation in our results we recognized that we could fill a knowledge gap by analyzing this precipitate.

Like the chelation described above, the precipitate may be a confounding variable when analyzing the effect of any IP in vitro. Not only does the physical presence of a precipitated complex alter the model system, but the precipitate may also trap components of the media, thereby altering the solubility of components in the extracellular environment. Additionally, the ability of the IP itself to interact with cells is limited as most of the IP will be trapped in insoluble precipitates. Viega and colleagues predict that less than 1 μM of $InsP_6$, and only a slightly higher concentration for $InsP_5$, will be soluble in any in vitro cell culture model (Veiga et al., 2006; Veiga et al., 2009). Because of these complexities, a portion of this thesis is devoted to disassociating our observed effect of vesicles formation from the confounding variable of precipitation by higher IPs.

1.4.3 Cellular internalization of *myo*-inositol phosphates and their rapid metabolism

The last two complexities of IP in vitro research will be discussed together as they are related and relevant to our discussion. First, because of their high negative charge density, IPs are unable to diffuse across the plasma membrane and into cells. The literature has also yet to identify a transporter for any IP. Several groups, however, have inferred the rapid internalization of radiolabeled $InsP_6$ by detecting its dephosphorylated products in range of cell lines post treatment with $InsP_6$ (Ferry et al., 2002; Vucenik & Shamsuddin, 1994; Windhorst et al., 2013). The current hypothesis is that higher IPs enter cells slowly through endocytosis via precipitated complexes (Brehm & Windhorst, 2019; Letcher et al.,

2008). Thus, applying cells exogenously in vitro may not result in a significant intracellular increase of that IP's concentration.

The last complexity is the rapid metabolism of any IP once it enters eucaryotic cells. Upon entering, most IPs, and certainly $InsP_6$, are quickly metabolized into dephosphorylated products (Irvine & Schell, 2001; Shears, 2001). Rapid metabolism, combined with slow cellular uptake, make it difficult to increase the intracellular pool of an exogenously applied IP. Here, our results are unique as both $InsP_5$ isomers we studied are not reported in eucaryotic metabolic pathways and thus may not be metabolizable by eucaryotic enzymes.

1.4 Vesicle formation in the endoplasmic reticulum

In our experiments we observed the formation of vesicles in the ER of human cancer cells in response to $InsP_6$ and $InsP_5$ treatment. To provide a framework for interpretating our results, we will provide a brief discussion on vesicle formation in the ER and several cellular events in which this phenotype has been reported.

Vesicles are spherical compartments made up of a lipid bilayer and a liquid interior (Cui et al., 2022). In animal cells, vesicles take part in secretion, transport, and digestion of intracellular components (Liu & Wang, 2023). Vesicles such as lysosomes and peroxisomes are specialized and have specific functions in digestion (Schrader et al., 2020). Vesicles are dynamic and often trafficked between the ER, Golgi apparatus and plasma membrane (Cui et al., 2022). They commonly form via endocytosis at the plasma membrane or budding from endomembrane components (Parkar et al., 2009).

The small diameter of most vesicles prevents their visualization by light microscopy (Mondal et al., 2019). However, in response to specific stimuli, vesicles can

fuse and enlarge to form giant vesicles that are visible by light microscopy. These larger structures are often termed vacuoles in the literature but will be referred to as vesicles in this thesis. The specific classification of these structures as vacuoles requires characterization not carried out in this thesis, therefore we will use the non-specific term vesicle. . The phrase 'vesicle formation' will also be used to describe the observation of enlarged vesicles. A common location for enlarged vesicles to be observed is in the ER. To date, several specific cellular events have been associated with vesicle formation in the ER. These events include disruption of ion and protein homeostasis, increased reactive oxygen species (ROS), ER stress, and plasma membrane injury (Raeymaekers & Larivière, 2011; Reggiori & Molinari, 2022b; Yoon et al., 2012). In general, the agents capable of inducing ER vesiculation are broad, and the phenotype itself is not indicative of one specific cellular process.

1.5 Research aims and objectives

A central goal of research conducted on *myo*-inositol phosphates is to understand their biological functions. Because of the collaboration by two laboratories in this project, we were uniquely positioned to extend this goal by investigating several relatively uncharacterized IPs. This thesis was the first project in either laboratory to investigate the effect of IPs on human cancer cells.

To summarize, my objectives were:

- To search for and identify phenotypic changes in human cancer cells upon treatment with both common and unique *myo*-inositol phosphates;
- To analyze the physiochemical properties of IP precipitates

- To investigate the potential role of the IP precipitate in the formation of the observed phenotype of vesicle formation

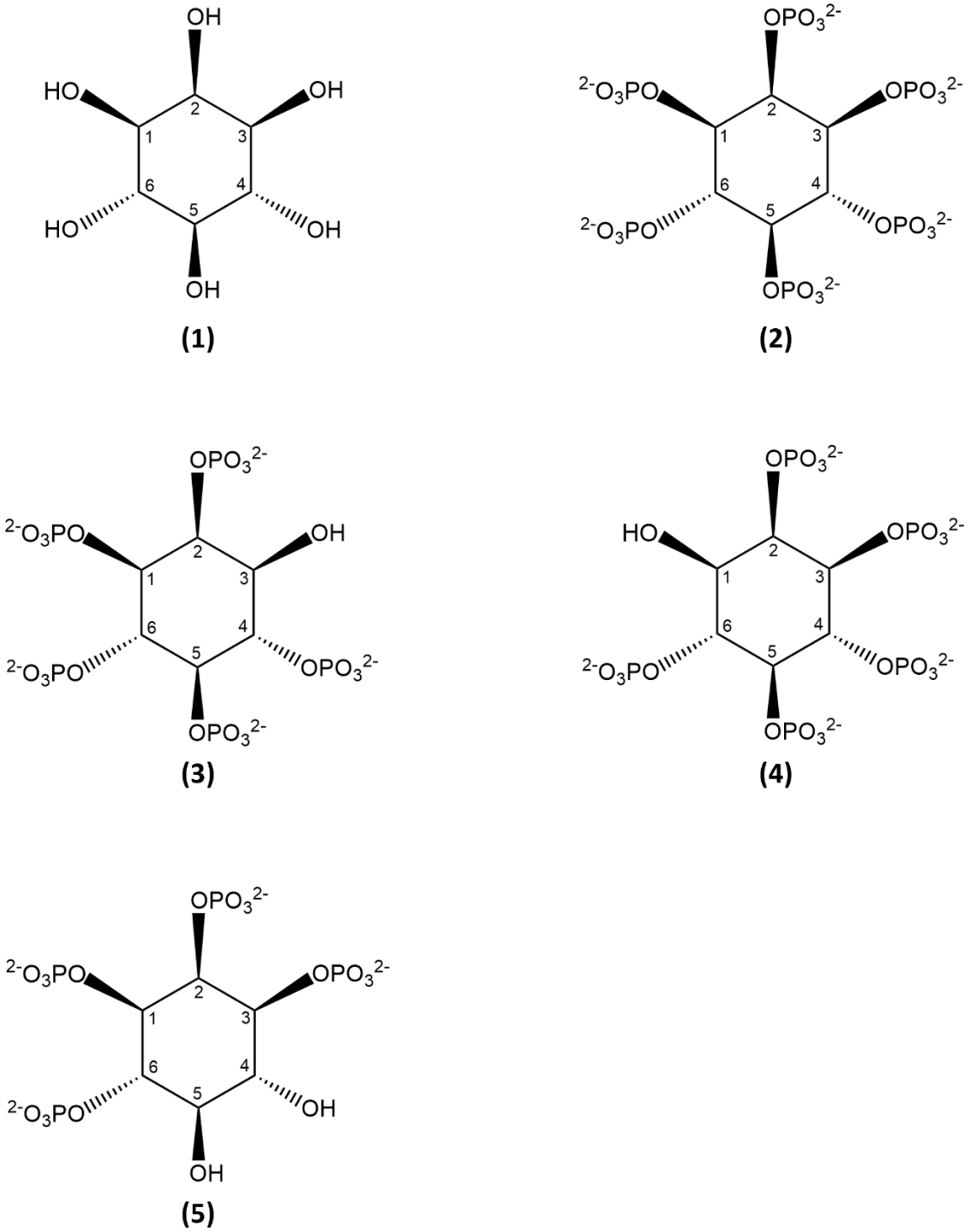

Figure 1.1 Chemical structures of *myo*-inositol and the four *myo*-inositol phosphates studied in this thesis. Structures were generated using ChemDraw 22.2.0 and are shown in their fully ionized states. Carbons are numbered using the D- configuration. *Myo*-inositol **(1)**, Ins(1,2,3,4,5,6)P_6 **(2)**, Ins(2,3,4,5,6)P_5 **(3)**, Ins(1,2,4,5,6)P_5 **(4)**, and Ins(1,2,3,4)P_4 **(5)**.

CHAPTER 2

Experimental Methods and Procedures

2.1 Cell culture

The human cell lines HT-29 (ATCC HTB-38) and U2OS (ATCC HTB-96) were obtained from the American Type Culture Collection (ATCC) and cultivated as previously described (Tuescher et al., 2021)**.** Briefly, the human cell line U2-OS was maintained in Dulbecco's Modified Eagle Medium (DMEM)/F-12 (Gibco; 11320-033) supplemented with 10% (v/v) heat-inactivated fetal bovine serum (FBS) (Gibco; 12484028), 2 mM Modified Eagle Medium non-essential amino acids (MEM-NEAA) (Gibco; 11140050), 1.6 mM GlutaMAX (Gibco; 35050-061), and 15 mM HEPES (4-(2-hydroxyethyl)-1-piperazineethanesulfonic acid), pH 7.4. The human cell line HT-29 was maintained in RPMI 1640 medium (Gibco; 21870-092) supplemented with 10% (v/v) heat-inactivated FBS (Gibco; 12484028) and 1.6 mM GlutaMAX (Gibco; 35050-061). Cells were grown at 37°C in 5% CO_2. U2-OS and HT-29 cells were plated at 5.0 x 10^5 cells/75 cm^2 flask and cultured for either 24 or 48 hours, respectively, prior to treatment. The following compounds were dissolved in dimethyl sulfoxide (DMSO; Sigma; D2438) and stored at -20 °C: Cyclosporine A (10 mM; Cayman Chemical; 59865-13-3) and Oleic acid (100 mM). The following compounds were dissolved in HyPure Molecular Biology Grade Water (HyClone; SH30538.02) and stored at 4°C: Deferoxamine (10 mM DFO; Sigma; D9533), Ethylene glycol bis-(2-aminoethyl ether)-N,N,N'N'-tetraacetic acid (100 mM EGTA; OmniPur; 4100), *myo*-inositol hexasulfate (12.5 mM $InsS_6$; Sigma; 28434-25-5), and *myo*-inositol hexakisphospahte (100 mM $InsP_6$; Sigma). $InsS_6$ and EGTA were solubilized by buffering with N-2-hydroxyethylpiperazine-N-2-ethane sulfonic acid (HEPES; Gibco;

15630-080). Ins(2,3,4,5,6)P_5, Ins(1,2,4,5,6)P_5, and Ins(1,2,3,4)P_4 were enzymatically derived, and their purity was assessed by MDD-HPIC chromatograms (appendix B).

2.2 Light microscopy

U2-OS and HT-29 cells were seeded at 2.0 x 10^4 cells per mL. Multi-well plates were prepared at 2 or 1 mL per well for 6- or 12- well plates, respectively, and incubated at 37°C prior to treatment. Cells were treated with either 1, 10, 30, or 100 µM of various IPs. If not otherwise specified, cells treated with IP isomers resulting in precipitation were washed twice with PBS and resuspended in media prior to imaging. Images were either captured with an Infinity 1 camera operated by Infinity Capture imaging software (Lumenera Corporation) on an Olympus CKX41 inverted microscope or a Cytation 5 cell imaging multi-mode reader (Biotek) operated by Gen 5 software (v 3.11). Images were processed using Microsoft PowerPoint 365 or ImageJ software (ImageJ; 1.50f) and experiments were performed three times.

2.3 Fluorescence microscopy

U2-OS cells were plated at 2.0 x 10^4 cells/mL of media into 6- or 12-well plates at 2 or 1 mL/well, respectively, and incubated at 37°C prior to treatment. Cells were incubated either with Nile red (Sigma; 72485), or 1X ER Cytopainter green (Abcam; 139481) for 15 minutes at 37°C. Cells were observed on a Cytation 5 (Biotek) microscope using either an Olympus UPlanFL N 20x objective with 0.45 numerical aperture or an Olympus UPlanFL N 40x objective with 0.60 numerical aperture. Images were captured using Gen5 software (v 3.11) for the Cytation 5 microscope. For both Nile Red and ER Cytopainter fluorescence was detected using the Green Fluorescent Protein filter cube (Biotek; 1225101; Ex:469/35 nm; Em:525/39 nm). Images were prepared using Microsoft PowerPoint 365 software and

ImageJ software (ImageJ; 1.50f). Percentage of cells with vesicles were counted manually and experiments were performed three times.

2.4 Localization of $InsP_6$ precipitate in cell culture

A unique protocol was utilized for localizing the precipitate to a specific region of cell culture flasks. U2-OS cells were placed in T25 flasks at a density of 5.0 x 10^5 cells/75 cm^2 and cultured for 24 hours prior to treatment. The total volume of media in the T25 flask was 5 mL. One corner nearest the opening of the T25 flask was designated as the precipitate corner (PPT corner). The corner diagonally across from the PPT corner was designated the non-PPT corner. $InsP_6$ was localized to the PPT corner by pipetting 15 µL of a 10 mM $InsP_6$ solution into that corner. The resulting concentration of $InsP_6$ throughout the T25 flask was 30 µM. Effort was taken to minimize mixing of the media prior to incubation. At 24 hours, both corners of the T25 flasks were visualized by light microscopy.

2.5 Pre-treatment of media with *myo*-inositol phosphates and removal of their precipitate prior to cell treatment

A unique protocol was developed for the removal of IP precipitates in media prior to cell treatment. U2-OS cells were seeded at 2.0 x 10^4 cells per mL in 12 well plates. U2-OS media (described above) was aliquoted by 1 mL fractions into 1.5 mL centrifuge tubes and pre-treated with IPs. These aliquots were left for at least 6 hours at room temperature to allow for precipitation of IPs with media components. The 1 mL aliquots were centrifuged for 5 minutes at 13000 rcf. Supernatants were decanted by careful pipetting, so as not to disturb the pelleted precipitate. Each supernatant was suspended on cells in 12 well plates 24 hours after plating. Cells were visualized by light microscopy 24 hours after treatment.

2.6 Detection of $InsP_6$ in precipitate by MDD-HPIC

Detection of $InsP_6$ in precipitate was performed by metal-dye detection high performance ion chromatography (MDD-HPIC). U2-OS media was divided into 1 mL aliquots and treated with either 100 or 1000 μM $InsP_6$. A third concentration of 10 μM was also tested requiring an aliquot of 10 mL to achieve a detectable signal. These aliquots were left for at least 15 minutes prior to centrifuging for 5 minutes at 13000 rcf. The supernatants were decanted. Pellets were resuspended in 2.5 % TCA and injected on to a MDD-HPIC system (HPIC; Waters 1525 Binary HPIC Pump; Milford, MA) utilizing a CarboPac PA-100 (4 x 240 mm) analytical column (Dionex; Sunnyvale, CA). $InsP_6$ was eluted with a methanesulfonic acid gradient and visualized using a post-column reactor with 0.1% (m/v) $Fe(NO_3)_3$ in a 2% (m/v) $HClO_4$ solution (0.3 mL/min).

2.7 Determination of precipitate in individual U2-OS media components

Individual components of U2-OS media were tested for the presence or absence of precipitate after treating 1 mL aliquots with 100 μM $InsP_6$. After 15 minutes, aliquots were centrifuged for 5 minutes at 13000 rcf and checked for the appearance of a visual white pellet. The appearance of a pellet was taken to represent the presence of precipitate in that aliquot. Complete U2-OS media (described above) and DMEM/F12 (Gibco; 11320-033) were tested directly. The remaining components were diluted with a 13 mM HEPES buffered solution to the concentrations they are present at within the complete U2-OS media. For example, FBS (Gibco; 12484028) was diluted to 10% v/v with 13 mM HEPES before testing. All other media components were generated artificially from inorganic salts.

2.8 Statistics

Data and statistical analyses were performed using Prism 10 software (GraphPad; 10.2.2) and data were plotted as means from three separate experiments ± standard errors of the means using Microsoft Excel 2016 software. Unpaired t-test analyses were performed on manual cell counts to calculate the statistically significant differences between two groups. One-way ANOVA with Tukey's post hoc analyses were performed on manual cell counts to calculate statistically significant differences between more than two group means.

CHAPTER 3

Results

3.1 $InsP_6$ induces precipitation in cell culture media and induces vesicles in U2-OS cells

U2-OS cells were treated with either H_2O (negative control) and observed by phase contrast microscopy at 24 h (Figure 3.1A). Cells treated with H_2O did not display any morphological changes, as expected. The percent of cells containing vesicles in H_2O treated cells was 1 %, which represents a baseline value (Figure 3.1B). U2-OS cells were also treated with either 1, 10, 30, or 100 μM $InsP_6$ and observed at 24 h by phase contrast microscopy (Figure 3.1A). Cells treated with 1 μM $InsP_6$ did not display any morphological change whereas cells treated with 10, 30, or 100 μM $InsP_6$ showed cytoplasmic vesicles. The percent of cells containing vesicles in 100 μM $InsP_6$ treated cells was 98 % (Figure 3.1B). The vesicles were light grey in color, circular, and clustered around the nucleus in the cytoplasm.

In the same experiment we also observed the formation of precipitate in wells treated with 10, 30, or 100 μM $InsP_6$ whereas wells treated with 1 μM $InsP_6$ showed no observable precipitate (Figure 3.1A). The amount of precipitate qualitatively appeared to increase with $InsP_6$ concentration. The quantity of precipitation in wells treated with 100 μM made it difficult to visualize the cells (Pre-wash). Consequently, cells were washed twice with PBS prior to visualizing (Wash). These experiments confirmed a previous observation in an undergraduate project that cells treated with $InsP_6$ appear to have vesicles and that $InsP_6$ precipitates in culture media at micromolar concentrations.

3.2 $InsP_6$ induced vesicles in HT-29 cells

After observing the $InsP_6$ induced vesiculated phenotype in U2-OS cells, we tested whether the same phenomenon would occur in a second cell line. HT-29 cells were treated with H_2O (negative control) and observed by phase contrast microscopy at 24 h. Prior to imaging, cells were washed twice with PBS. Cells treated with H_2O did not show any morphological change, as expected (Figure 3.2). HT-29 cells were also treated with either 10, 30, or 100 μM $InsP_6$ and observed by phase contrast microscopy at 24 h. Cells were then washed twice with PBS to remove precipitate prior to imaging. Cells treated 10 μM $InsP_6$ appeared normal whereas cells treated with 30 or 100 μM $InsP_6$ showed vesicles (Figure 3.2). This confirms that $InsP_6$ can induce vesicles in a second cell line and that the vesicle phenotype is a broad biological phenomenon. Even though U2-OS and HT-29 cells are both of epithelial origin, the apical polarity of the HT-29 cells made it difficult to observe the vesicles in this cell line. Thus, U2-OS cells were used for all future experiments.

3.3 The observed precipitate contains $InsP_6$ and inorganic cations from cell culture media

At this point we have observed that $InsP_6$ produces two effects when exogenously applied to cultured cells: first, precipitation within culture media, and second, vesicles within cells. We first sought to characterize the nature of the observed precipitate. $InsP_6$ is capable of precipitating with cations like calcium, zinc, iron and magnesium (Odani et al., 2011; Vasca et al., 2002). We sought to determine if $InsP_6$-cation interactions were indeed the source of precipitation in cell culture media. To do this we took U2-OS cell culture media components and added $InsP_6$ to a concentration of 100 μM and asked if a precipitate

had formed or not. To aid in detecting precipitation, the mixtures were centrifuged and then checked for the formation of a white pellet (the precipitate). We tested the components of U2-OS culture media, DMEM/F12 and FBS, separately. We observed precipitate in DMEM/F12 treated with 100 μM $InsP_6$, whereas no precipitate was observed in FBS (Table 3.2). The individual components of DMEM/F12 can be categorized as amino acids, vitamins, inorganic salts, and other components (i.e. phenol red, lipids, or additives). We chose to test the inorganic salt component first because it is the source of cations in DMEM/F12 known to precipitate with $InsP_6$ (Thermo Fisher, 2024).We observed precipitate in the inorganic salt component treated with 100 μM $InsP_6$ (Table 3.2). The other components were not tested since they do not contain substrates likely to precipitate with $InsP_6$.

Of the cations present in the inorganic salt component of DMEM/F12, calcium and magnesium are the most probable precipitate constituents given that all other cations are present at trace concentrations (Table 3.1). Only calcium and magnesium are present above 10-100 μM, the concentrations of $InsP_6$ where precipitate was observed in media. We therefore prepared the inorganic salt solutions as one without calcium and the other without magnesium. We observed precipitate in the magnesium free solution treated with 100 μM $InsP_6$, whereas no precipitate was observed in the calcium free solution treated with 100 μM $InsP_6$. We next treated a 1 mM calcium solution, pH 7.2, with 100 μM $InsP_6$ and observed precipitate. We reasoned that if calcium is the source of precipitation with $InsP_6$, we expect the prior treatment of the inorganic salt solution with EGTA, a cation chelator with high affinity for calcium (Rothen-Rutishauser et al., 2002; Takadera et al., 2010), to prevent precipitation. We thus pretreated the original 1 mM calcium solution with 2 mM

of EGTA to chelate all available calcium prior to addition of $InsP_6$ and observed no precipitate when treated with 100 μM $InsP_6$ (Table 3.2). These results suggest that calcium is necessary for the observed $InsP_6$ precipitate U2-OS cell culture media.

To test further the hypothesis that the precipitate is a metal-IP complex we asked if $InsP_6$ was present in the precipitate by a metal-dye detection high-pressure ion chromatography (MDD-HPIC) system. Media treated with 10, 100 or 1000 μM $InsP_6$ showed 67, 123 and 52 % of total $InsP_6$ in the precipitate, respectively (Figure 3.3). The fact that $InsP_6$ was detected in all precipitates at all concentrations tested qualitatively confirms the presence of $InsP_6$ in the precipitate observed within U2-OS media. Therefore, these combined results indicate that $InsP_6$ and calcium are substantial components of the observed precipitate in culture media.

3.4 Physical contact of visible $InsP_6$ induced precipitate with cells is not required for the vesiculated phenotype

Having noted that the precipitate appeared to be in physical contact, or at least in proximity with the cells and that the presence of precipitate appears correlated with the appearance of vesicles we considered the precipitate itself as a potential confounding variable. Physical contact of precipitate, specifically calcium-phosphate precipitate (CCP), with cell monolayers has been reported to affect human cells (Chen et al., 2014; Gao et al., 2008). Thus, we designed an experiment to determine if physical contact by the precipitate with cultured cells is necessary for the vesiculated phenotype.

The heavy, bulky nature of the precipitate made it possible to control its distribution throughout a tissue culture flask. We applied 100 μM to a specific region of the flask rather

than distributing the $InsP_6$ evenly. The corner where the $InsP_6$ was pipetted was designated as the precipitate corner (PPT corner) while the corner furthest away from where the $InsP_6$ was pipetted was designated the non-precipitate corner (non-PPT corner). The cells were observed by phase contrast microscopy for 24 h. Images taken in the PPT corner show dark precipitate above the cells, whereas images taken in the non-PPT corner show no precipitate present (Figure 3.4A). Cells observed in the both the PPT corner and non-PPT corner show vesicles. (Figure 3.4A). The percent of cells containing vesicles in the PPT corner and non-PPT corner was 100 ± 0 and 95 ± 5 %, respectively (Figure 3.4B). These data indicate that physical contact of the $InsP_6$ precipitate is not required for vesicle formation in U2-OS cells and that their formation is dependent on a soluble component.

3.5 The pre-treatment of media with $InsP_6$ and subsequent removal of the $InsP_6$ precipitate maintains the vesiculated phenotype

Since vesicle formation occurs via the soluble portion of the media, we hypothesized that treatment of IP_6 with culture media may modify its composition (specifically the solubility of specific cations) and that this media modification may be the cause of the vesiculated phenotype. To test this, we designed an experiment where U2-OS culture media was either not treated or pre-treated with 100 μM IP_6 and left for 6 h to allow for precipitation of the $InsP_6$. Both treatments were then centrifuged to remove all precipitate and cells were treated with the media supernatants of both treatments. Cells treated with the 100 μM $InsP_6$ supernatant showed vesicles whereas cells treated with the un-treated supernatant showed no vesicles (Figure 3.5A). The percent of cells containing vesicles in wells treated with the 100 μM $InsP_6$ supernatant and the un-treated supernatant was 77 ± 13 and 0 ± 0 %, respectively (Figure 3.5B). These results indicate that formation

of $InsP_6$ precipitate modifies the culture media, and that the presence of insoluble precipitate in the culture media is not required for vesicle formation.

3.6 EGTA and DFO do not induce vesicle formation in U2-OS cells

Suspecting cation depletion in the media to be a potential cause of vesicle formation, we tested whether EGTA would produce the same effect. U2-OS cells were treated with H_2O (negative control) or 30 μM $InsP_6$ (positive control) and observed by phase contrast microscopy at 24 h (Figure 3.6). Cells treated with H_2O did not show any morphological change whereas cells treated with 30 μM $InsP_6$ showed vesicles, as expected (Figure 3.6). U2-OS cells were also treated with either 100, 500, 1000, or 1500 μM EGTA and observed at 24 h by phase contrast microscopy. Cells treated with EGTA showed no vesicles or precipitation at all concentrations tested (Figure 3.6). Notably, cells treated with 1 and 1.5 mM EGTA showed disassembled cell-cell contacts, and at 1.5 mM EGTA alone, detachment from the culture flask (Figure 3.6). These results suggest that extracellular calcium depletion is not sufficient to cause the vesicle formation induced by $InsP_6$.

Given reports that $InsP_6$ decreases iron absorption in vitro and in vivo (Glahn et al., 2002; Hoes et al., 2018; Hurrell & Egli, 2010; Ma et al., 2011) we also tested deferoxamine (DFO), a synthetic iron chelator, at concentrations known to induce iron depletion in vitro (Hoes et al., 2018). Cells were treated with either H_2O (negative control) or 30 μM $InsP_6$ (positive control) and observed by phase contrast microscopy at 24 h. Cells treated with H_2O did not show any morphological change whereas cells treated with 30 μM $InsP_6$ showed vesicles, as expected (Figure 3.7). U2-OS cells were also treated with either 10, 30, or 100 μM DFO and observed at 24 h by phase contrast microscopy. Cells treated with DFO showed no vesicles or precipitation at all concentrations tested (Figure 3.7). These

results indicate that iron depletion is not sufficient to cause the $InsP_6$ induced vesicle formation. While the mechanism behind vesicle induction by $InsP_6$ appears to be modification of the extracellular media, the extracellular cation chelators EGTA and DFO do not induce the same vesicle effect.

3.7 Ins(1,2,4,5,6)P_5 and Ins(2,3,4,5,6)P_5 induce precipitate in cell culture media and vesicles in U2-OS cells whereas Ins(1,2,3,4)P_4 does neither

Because of the chemical similarity between $InsP_6$ and several of our enzymatically derived IP isomers (Figure 1.1) we hypothesized that other IPs may be able to induces vesicle and the associated precipitation in cell culture. IPs are similar in that they all contain high negative charge density, especially the higher phosphorylated IPs. Previous research in our laboratory gave us unique access to IP isomers to answer this question. The two $InsP_5$ isomers we tested have not been published as metabolic products in eucaryotes and are likely not naturally present in human cells. We treated U2-OS with H_2O (negative control) and observed them by phase contrast microscopy at 24 h. Cells treated with H_2O did not show any morphological change, as expected (Figure 3.8A). U2-OS cells were also treated with either 1, 10, or 100 μM of either Ins(1,2,4,5,6)P_5, Ins(2,3,4,5,6)P_5, or Ins(1,2,3,4)P_4 and observed for 24 h by phase contrast microscopy. Cells treated with 1, 10, or 100 μM Ins(1,2,3,4)P_4 showed no vesicles formation (Figure 3.8A). Additionally, for all concentrations of Ins(1,2,3,4)P_4 no precipitate was observed by light microscopy. Cells treated with 1 μM of either Ins(1,2,4,5,6)P_5 or Ins(2,3,4,5,6)P_5 also showed no vesicles whereas cells treated with 10 or 100 μM of either Ins(1,2,4,5,6)P_5 or Ins(2,3,4,5,6)P_5 showed vesicles (Figure 3.8A). Precipitate was also observed in the cell culture at both 10 and 100 μM of Ins(1,2,4,5,6)P_5 and Ins(2,3,4,5,6)P_5. The percent of cells

with vesicles treated with 100 μM Ins(2,3,4,5,6)P_5 or Ins(1,2,4,5,6)P_5 was 97 ± 4 and 98 ± 2 %, respectively, whereas cells treated with 100 μM Ins(1,2,3,4)P_4 showed 1 ± 1 % vesiculated cells (Figure 3.8B). Together, these results indicate that two $InsP_5$ isomers form precipitates in cell culture media and induce vesicles, similar to those induced by $InsP_6$, whereas a lower phosphorylated $InsP_4$ isomer neither formed precipitate nor induced vesicles at the tested concentrations.

3.8 The pre-treatment of media with Ins(2,3,4,5,6)P_5 and subsequent removal of the Ins(2,3,4,5,6)P_5 precipitate maintains the vesiculated phenotype.

Having observed that two $InsP_5$ isomers both induced a phenotypic effect similar as that of $InsP_6$ on U2-OS cells, we then asked whether Ins(2,3,4,5,6)P_5 in place of $InsP_6$, would form a precipitate, that when removed, would have a similar vesicle effect as $InsP_6$. U2-OS culture media was pre-treated with either 100 μM Ins(2,3,4,5,6)P_5 or left untreated and let rest for 6 h to allow for precipitation of the Ins(2,3,4,5,6)P_5. Both samples were then centrifuged to remove precipitate and cells were treated with the media supernatants of both treatments. Cells treated with the 100 μM Ins(2,3,4,5,6)P_5 supernatant showed vesicles whereas cells treated with the un-treated supernatant showed no vesicles (Figure 3.9A). The percent of cells containing vesicles in wells treated with the 100 μM Ins(2,3,4,5,6)P_5 supernatant and the un-treated supernatant was 100 ± 0 and 0 ± 0 %, respectively (Figure 3.9B). These results indicate that, like IP_6, Ins(2,3,4,5,6)P_5 modifies the culture media, and that this modification is responsible for the vesiculated phenotype.

3.9 $InsS_6$ does not induce precipitation in cell culture media nor induce vesicles in U2-OS cells

We asked if inositol hexasulphate ($InsS_6$), a structural analog of $InsP_6$, could also produce a similar vesicle and precipitate phenotype (Shears, 2001). Due to its similar structure and negative charge, $InsS_6$ is often used as an isosteric, non-physiological analog of $InsP_6$ and has been shown to have similar interactions as $InsP_6$ to various biomolecules (Cecconi et al., 1994; Larsson et al., 1997; Ullah & Sethumadhavan, 1998). U2-OS cells were treated with either H_2O (negative control) or 100 μM $InsP_6$ (positive control) and observed at 24 h by phase contrast microscopy. Cells treated with H_2O (negative control) appeared normal whereas cells treated with 100 μM IP_6 (positive control) appeared vesiculated (Figure 3.10). Cells were also treated with either 100, 300, or 1000 μM $InsS_6$ and observed at 24 h by phase contrast microscopy. Cells treated with 100, 300, 1000 μM $InsS_6$ appeared normal (Figure 3.10). No precipitate was observed in any well treated with $InsS_6$. These results indicate that despite the structural similarity of $InsS_6$ with $InsP_6$, it does not precipitate in culture media nor induce vesicles in U2-OS cells.

3.10 $InsP_6$ induced vesicles are not lipophilic

Next, we sought to characterize the nature and origin of the vesicles. Previous studies report that vesicles observed adjacent to the nucleus may be lipid droplets associated with the endoplasmic reticulum (ER) (Lee et al., 2015). To test whether the $InsP_6$ induced vesicles were lipid droplets we used the lipophilic stain, Nile Red, which selectively fluoresces green in lipid-rich environments (Greenspan et al., 1985). We treated U2-OS cells with either H_2O (negative control) or 100 μM Oleic acid (positive control), which induces lipid droplets (Brasaemle et al., 1997). H_2O treated cells appeared normal

by phase contrast microscopy at 24 h with no observable green fluorescence by fluorescence microscopy (Figure 3.11). Oleic acid treatment resulted in vesicles, some of which appeared bright white, adjacent to the nucleus, as observed by phase contrast microscopy and green fluorescence was observed localized to these vesicles by fluorescence microscopy (Figure 3.11). U2-OS cells were also treated with 100 μM $InsP_6$. $InsP_6$ treated cells showed vesicles surrounding the nucleus by phase contrast microscopy and no observable green fluorescence by fluorescence microscopy (Figure 3.11). Interestingly, unlike the Oleic acid induced vesicles, the $InsP_6$ induced vesicles did not appear bright white by phase contrast microscopy, but instead appeared grey. These results revealed that the $InsP_6$ induced vesicles are not lipid droplets.

3.11 $InsP_6$ induced vesicles are localized to the endoplasmic reticulum

Having observed that the vesicles induced by $InsP_6$ are found adjacent to the nucleus, we hypothesized that they may originate from the ER. To test this, we used cyclosporine A (CsA), an inducer of vesicles in the ER as a positive control (Ram & Ramakrishna, 2014; Zupanska et al., 2005). We sought to compare the vesicles induced by CsA, known to be in the ER, with the vesicles produced by $InsP_6$. We used an ER membrane specific dye, ER Cytopainter, to observe the membrane structure of the ER. U2-OS cells were treated with either H_2O (negative control) or 30 μM CsA (positive control) observed by phase contrast and fluorescence microscopy at 24 h. We observed that cells treated with H_2O appeared normal by phase contrast microscopy with the ER Cytopainter fluorescence localized to the perinuclear region by fluorescence microscopy (Figure 3.12). Cells treated with CsA showed a vesiculated phenotype throughout the perinuclear region by phase contrast microscopy and a dispersed ER Cytopainter signal delineating the

vesicles observed by fluorescence microscopy (Figure 3.12). U2-OS cells were also treated with 100 μM $InsP_6$ and observed at 24 h by phase contrast and fluorescence microscopy. $InsP_6$ treated cells showed vesicles surrounding the nucleus by phase contrast microscopy and a dispersed ER Cytopainter signal delineating the vesicles observed by fluorescence microscopy (Figure 3.12). These results suggest that the vesicles induced by $InsP_6$ are localized to the ER, like the vesicles induced by CsA.

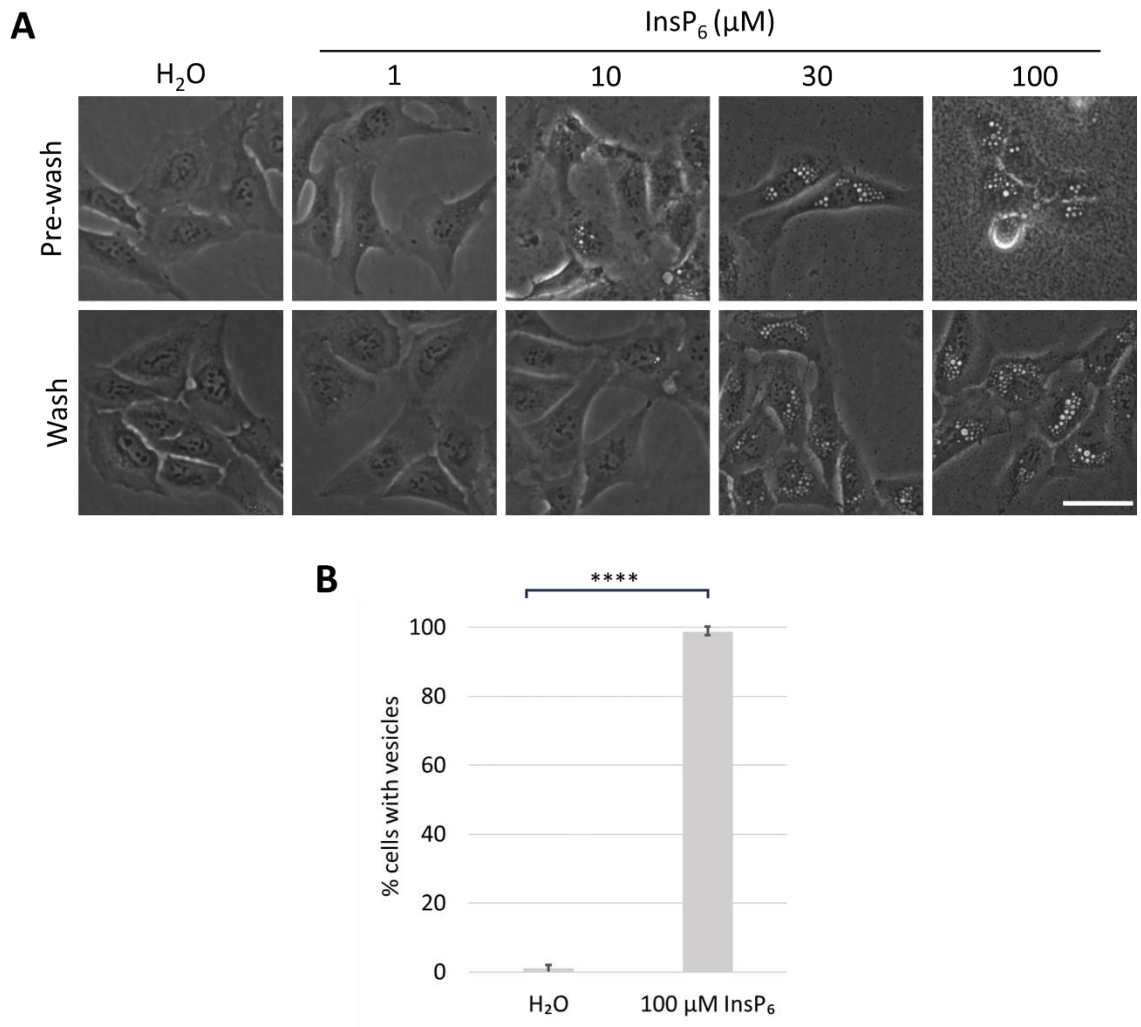

Figure 3.1 $InsP_6$ produces precipitation in cell culture media and induces vesicle formation in U2-OS cells. **(A)** U2-OS cells were treated with either H_2O, 1, 10, 30 or 100 μM $InsP_6$ and imaged at 24 h by phase contrast microscopy. The bottom (Wash) panel indicates images taken post washing with PBS. The top (Pre-wash) panel indicates cells imaged prior to the PBS wash. Scale bar = 50 μm. **(B)** Cells treated with either H_2O or 100 μM IP_6 were counted manually using ImageJ software and percent vesiculated cells were calculated from three experiments. Values are means and error bars represent SEM. (**** $p<0.0001$).

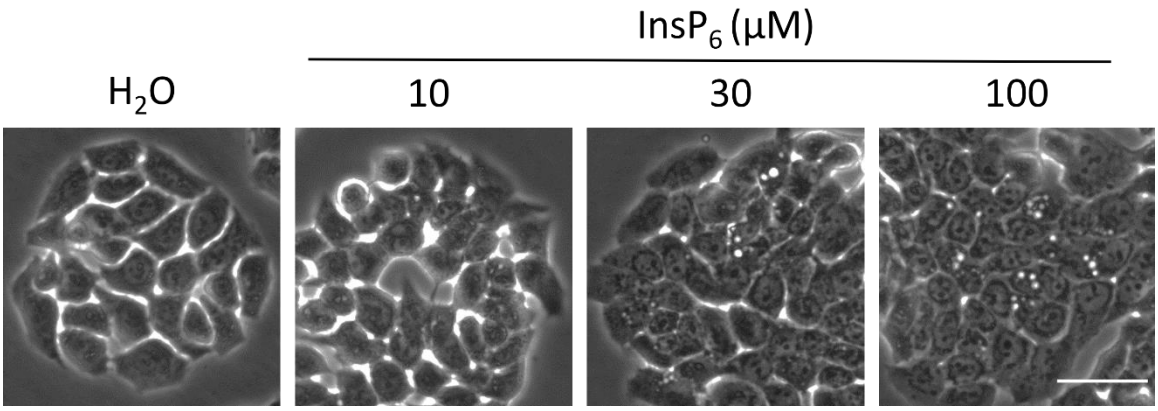

Figure 3.2 $InsP_6$ induces vesicle formation in HT-29 cells. HT-29 cells were treated with either H_2O, 10, 30 or 100 μM $InsP_6$ and imaged at 48 h by phase contrast microscopy. Scale bar = 50 μm.

Table 3.1 Concentrations of all inorganic salts in DMEM/F12 (Gibco; 11320-033)(ThermoFisher, 2024).

Inorganic Salt	(mg/mL)	(mM)
Calcium Chloride	116.6	1.05
Cupric Sulfate	0.0013	0.5E-5
Ferric Nitrate	0.05	1.24
Ferric Sulfate	0.417	0.2E-2
Magnesium Chloride	28.64	0.30
Magnesium Sulfate	48.84	0.41
Zinc Sulfate	0.432	0.2E-2

Table 3.2 Presence or absence of $InsP_6$ precipitate in individual components of U2-OS cell culture media. Aliquots of each media component were treated with 100 μM $InsP_6$ prior to centrifuging and pellet collection. The formation of a white pellet was taken to represent presence of precipitate.

U2OS Media Component	Precipitate
U2OS Complete Media	+
DMEM/F12	+
FBS	-
DMEM/F12 Inorganic Salts	+
DMEM/F12 Inorganic Salts (- Mg^{2+})	+
DMEM/F12 Inorganic Salts (- Ca^{2+})	-
1 mM $CaCl_2$, pH 7.2	+
2 mM EGTA, 1 mM $CaCl_2$, pH 7.2	-

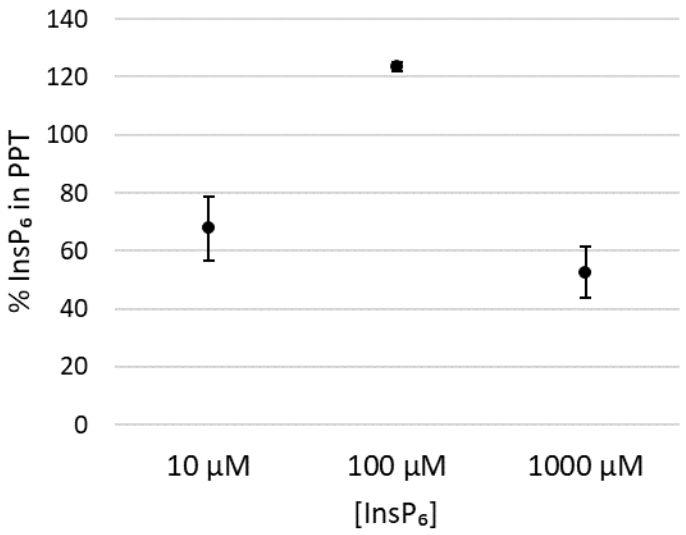

Figure 3.3 $InsP_6$ is present in the precipitate observed upon $InsP_6$ addition to U2-OS culture media. Media aliquots were treated with either 10, 100 or 1000 µM $InsP_6$ prior to centrifuging and pellet collection. Pellets were resuspended in 2.5 % TCA and analyzed by MDD-HPIC. Values are means of three replicates and error bars represent SEM.

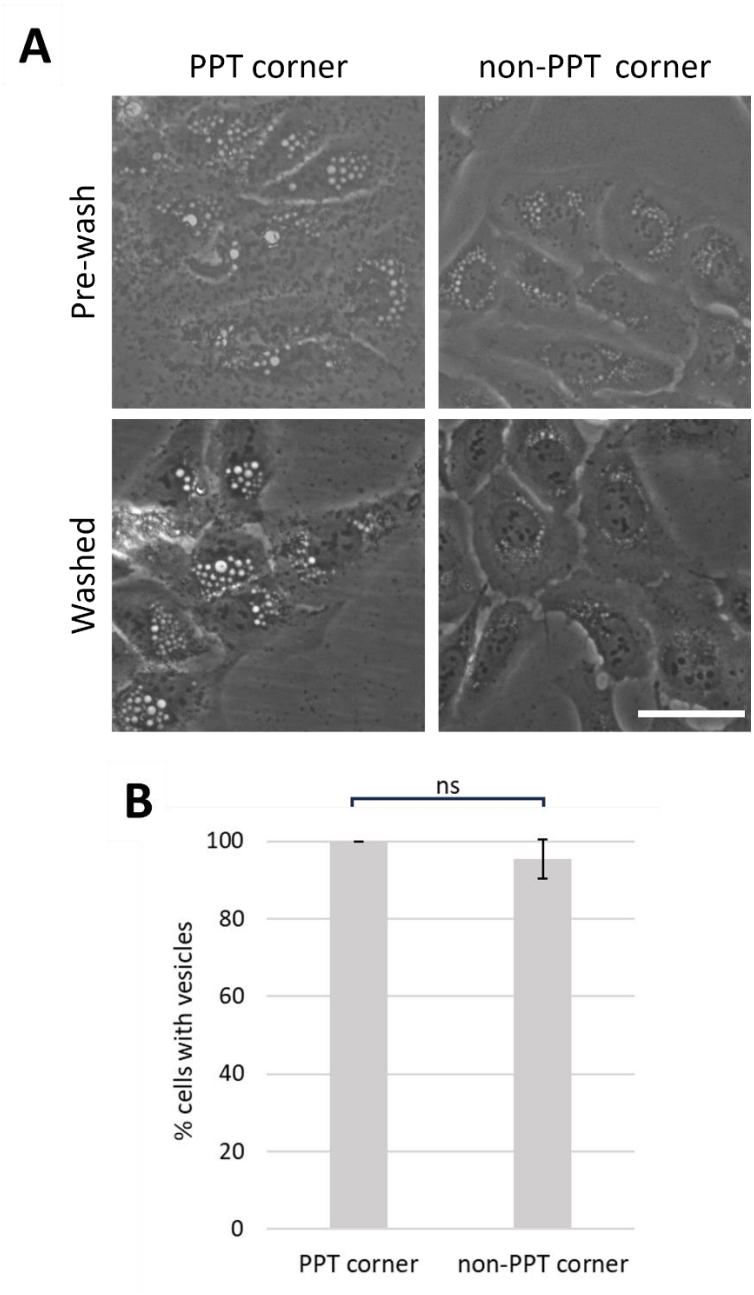

Figure 3.4 Physical contact of the $InsP_6$ precipitate with cells is not required for the vesiculated phenotype. **(A)** U2-OS cells were treated in T25 flasks with 30 µM $InsP_6$. The $InsP_6$ precipitate was localized to a specific corner of the flask, designated the PPT corner. Cells were imaged at 24 h by phase contrast microscopy. The bottom (Washed) panel indicates images taken post washing with PBS. The top (Pre-wash) panel indicates cells imaged prior to the PBS wash. Scale bar = 50 µm. **(B)** Cells in both corners were counted manually using ImageJ software and percent vesiculated cells were calculated from three experiments. Values are means and error bars represent SEM. (ns p=0.1836).

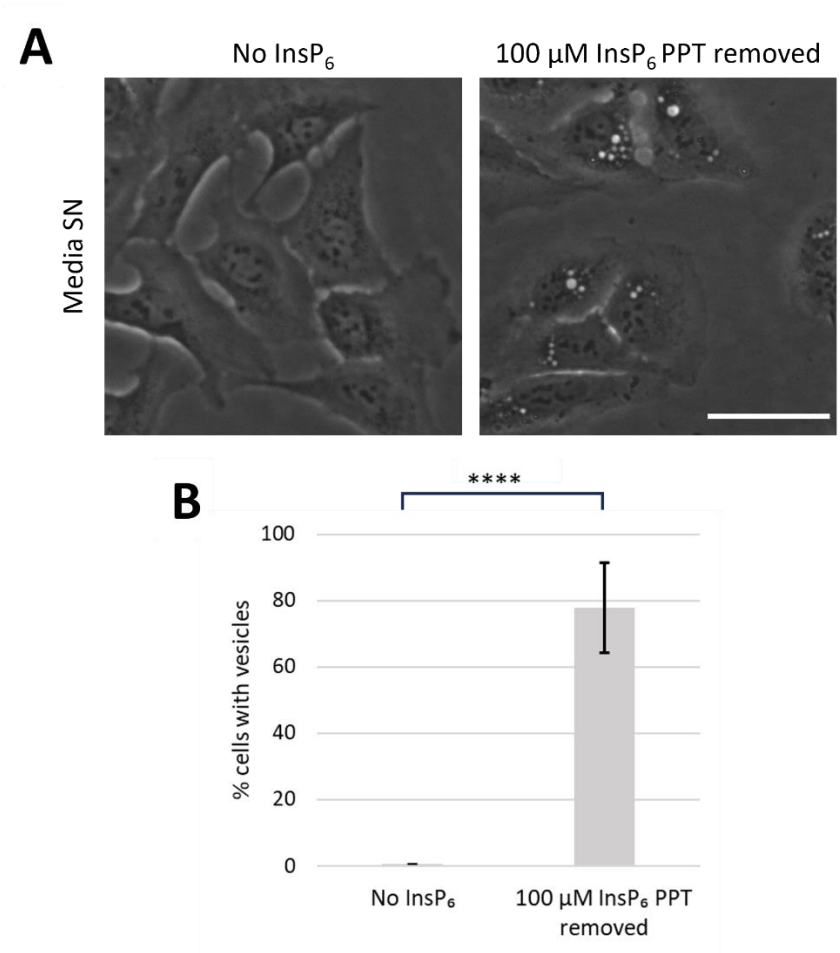

Figure 3.5 The pre-treatment of U2-OS media with $InsP_6$ and subsequent removal of the $InsP_6$ precipitate maintains the vesiculated phenotype. **(A)** U2-OS culture media was either untreated or pretreated with 100 µM $InsP_6$ and left for 6 h prior to precipitate removal by centrifugation. U2-OS cells were treated with both supernatants and imaged at 24 h by phase contrast microscopy. Scale bar = 50 µm. **(B)** Cells in both treatments were counted manually using ImageJ software and percent vesiculated cells were calculated from three experiments. Values are means and error bars represent SEM. (**** $p<0.0001$)

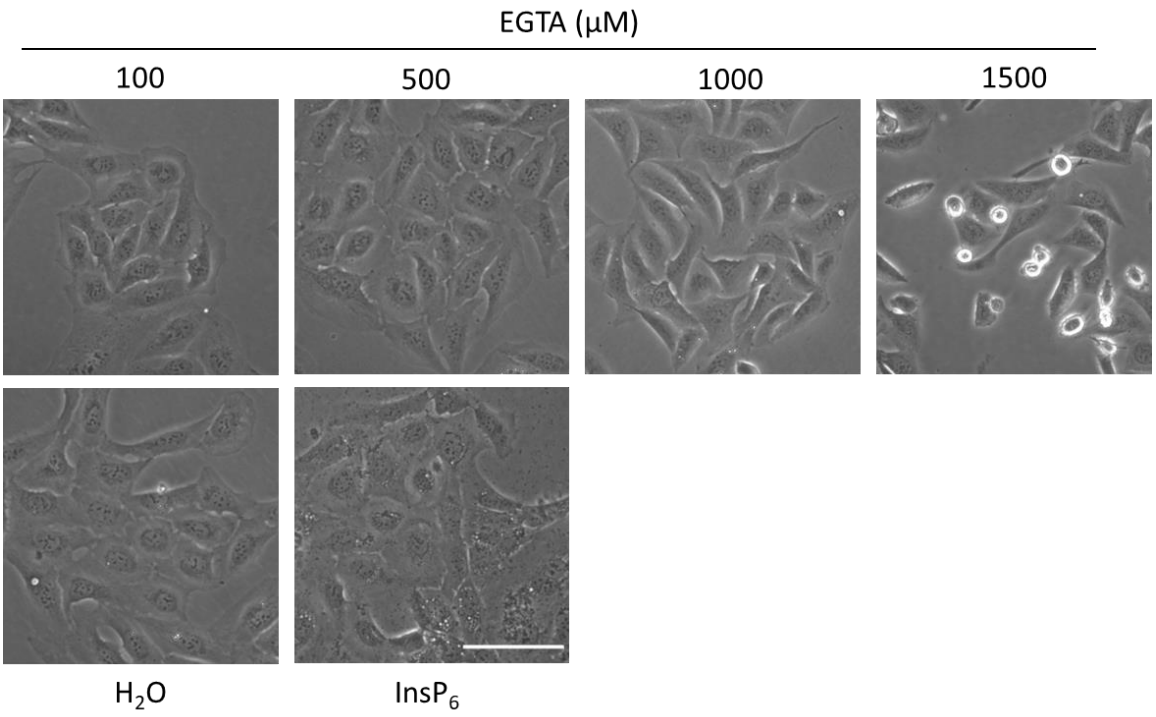

Figure 3.6 EGTA does not induce vesicles like those induced by $InsP_6$. U2-OS cells were treated with either H_2O or 30 μM $InsP_6$ or either 100, 500, 1000, or 1500 μM EGTA. Cells were imaged at 24 h by phase contrast microscopy. Scale bar = 100 μm.

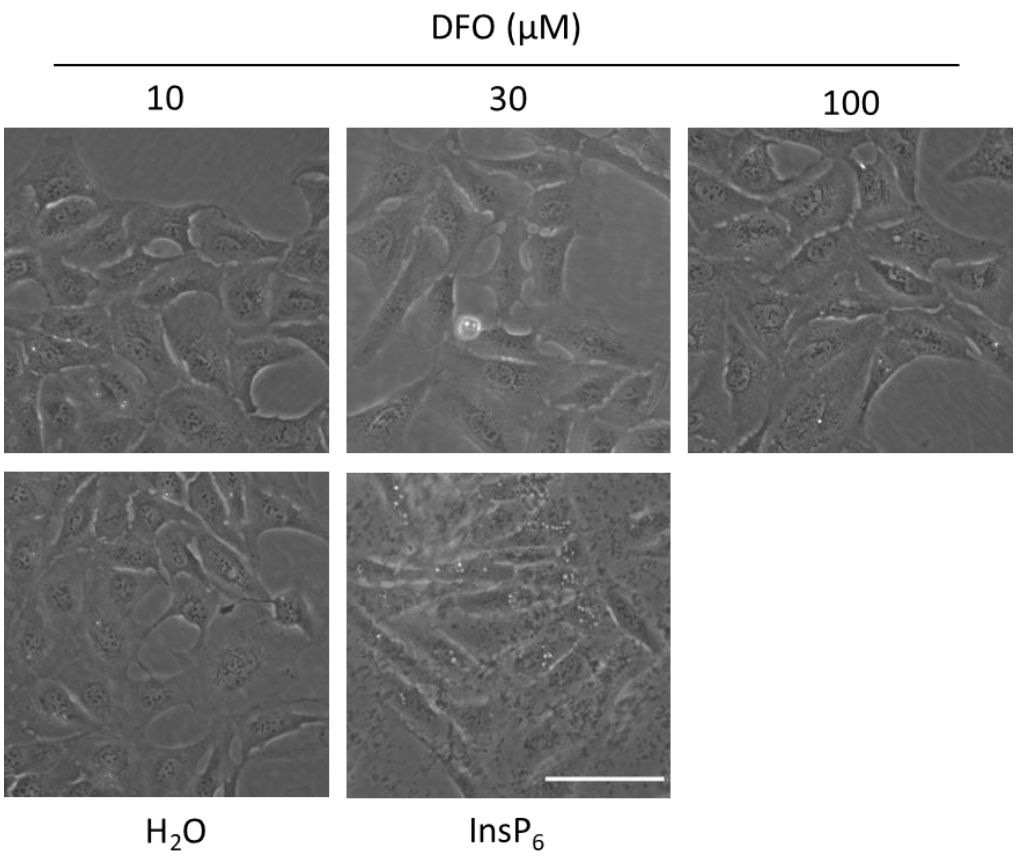

Figure 3.7 DFO does not induce vesicles like those induced by $InsP_6$. U2-OS cells were treated with either H_2O or 30 μM $InsP_6$ or either 10, 30, or 100 μM DFO. Cells were imaged at 24 h by phase contrast microscopy. Scale bar = 100 μm.

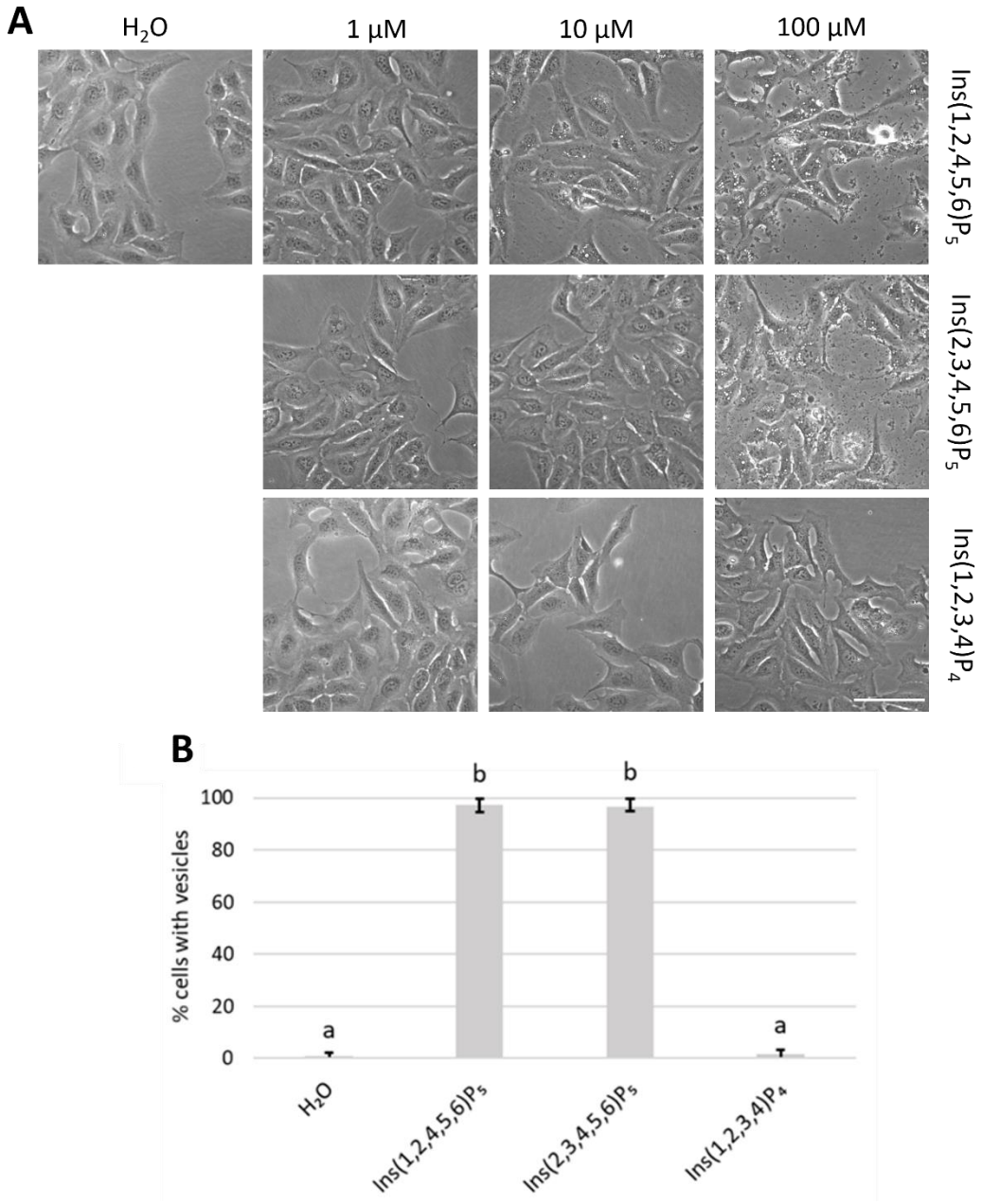

Figure 3.8 Ins(1,2,4,5,6)P_5 and Ins(2,3,4,5,6)P_5 induce precipitate in culture media and vesicles in U2-OS cells, respectively, whereas Ins (1,2,3,6)P_4 does neither. **(A)** U2-OS cells were treated with H_2O or either 1, 10 or 100 of Ins(1,2,3,4)P_4, Ins(2,3,4,5,6)P_5 or Ins(1,2,4,5,6)P_5. Cells were imaged at 24 h by phase contrast microscopy. Scale bar = 100 µm. **(B)** Cells treated with H_2O and 100 µM of each IP were counted manually using ImageJ software and percent vesiculated cells were calculated from three experiments. Values are means and errors bars represent SEM. Statistical significance was determined using one-way ANOVA followed by Tukey's post hoc test ($p < 0.0001$). Means that are significantly different from the mean of the H_2O treatment are represented with a different letter (a, b).

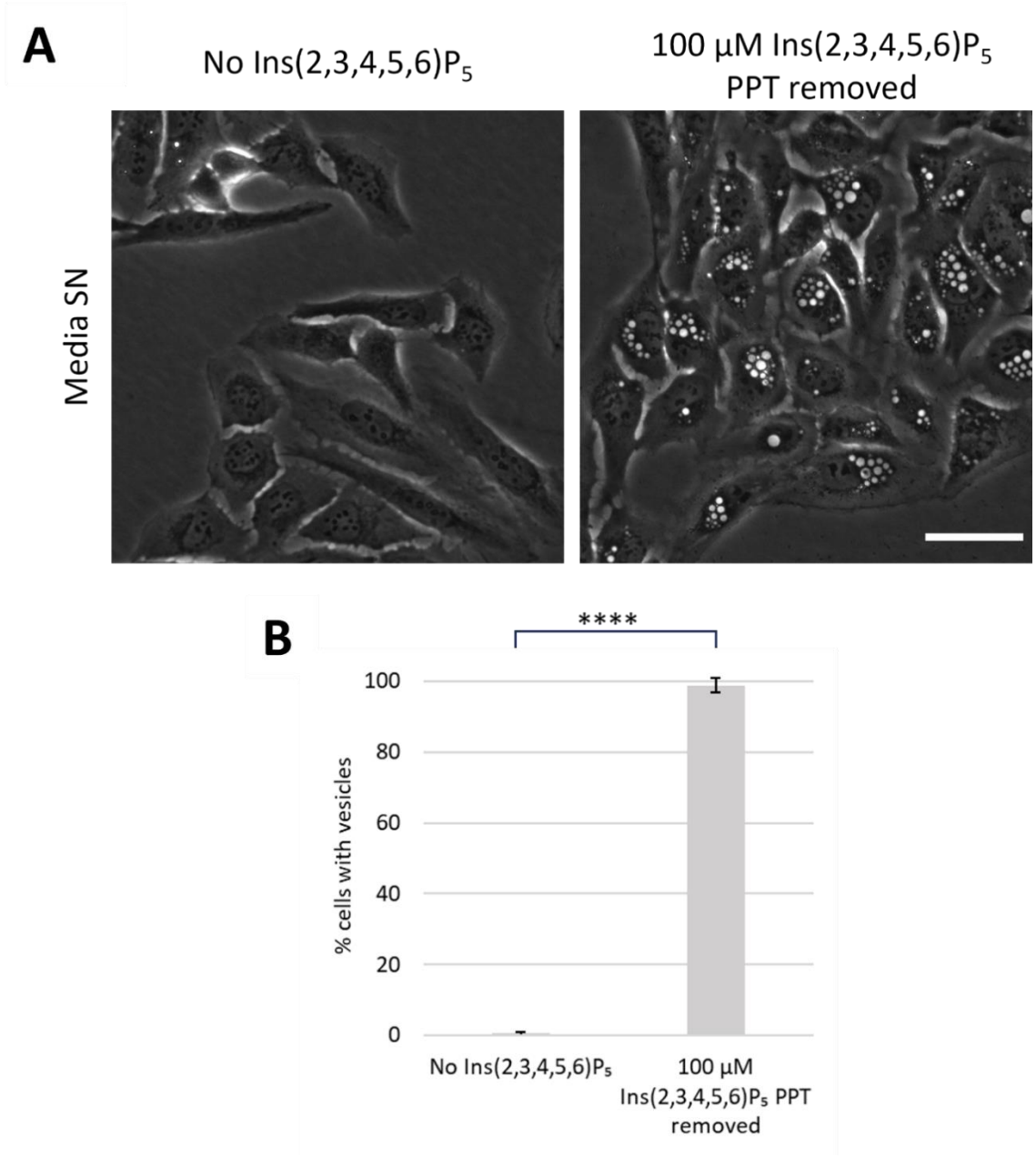

Figure 3.9 The pre-treatment of U2-OS media with Ins(2,3,4,5,6)P_5 and subsequent removal of the Ins(2,3,4,5,6)P_5 precipitate maintains the vesiculated phenotype. **(A)** U2-OS culture media was either untreated or pretreated with 100 µM Ins(2,3,4,5,6)P_5 and left for 6 h prior to precipitate removal by centrifugation. U2-OS cells were treated with both supernatants and imaged at 24 h by phase contrast microscopy. Scale bar = 50 µm. **(B)** Cells in both treatments were counted manually using ImageJ software and percent vesiculated cells were calculated from three experiments. Values are means and error bars represent SEM. (**** $p<0.0001$).

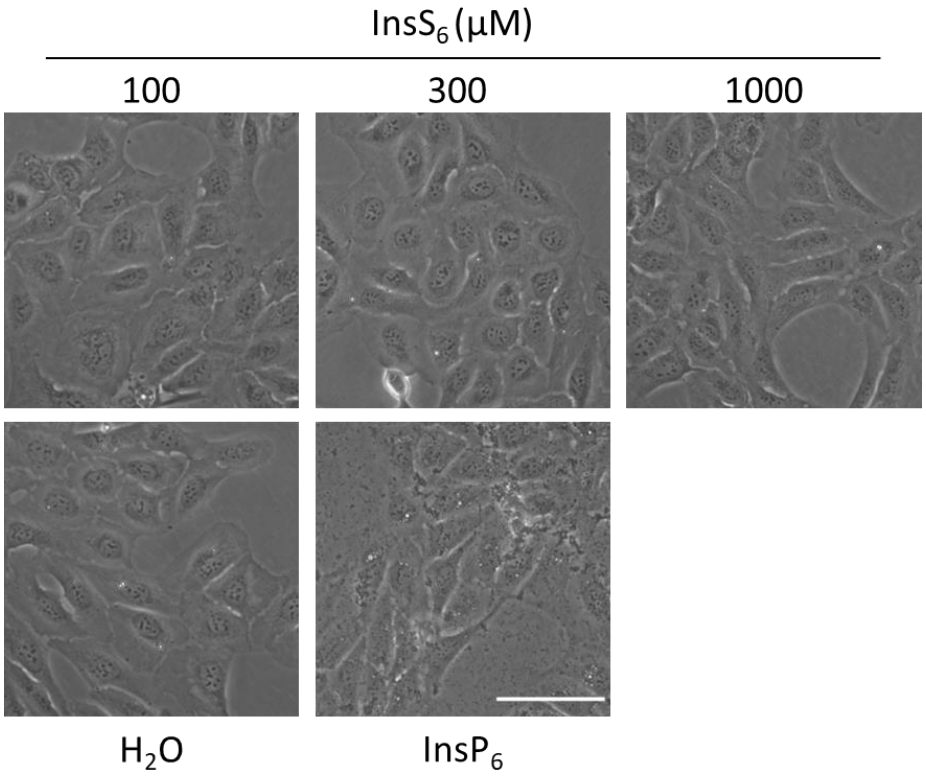

Figure 3.10 $InsS_6$ does not induce precipitate in culture media nor vesicles U2-OS cells, respectively. Cells were treated with either H_2O, 30 μM $InsP_6$, or either 100, 300, or 1000 μM $InsS_6$ and observed for 24 h by phase contrast microscopy. Scale bar = 100 μm.

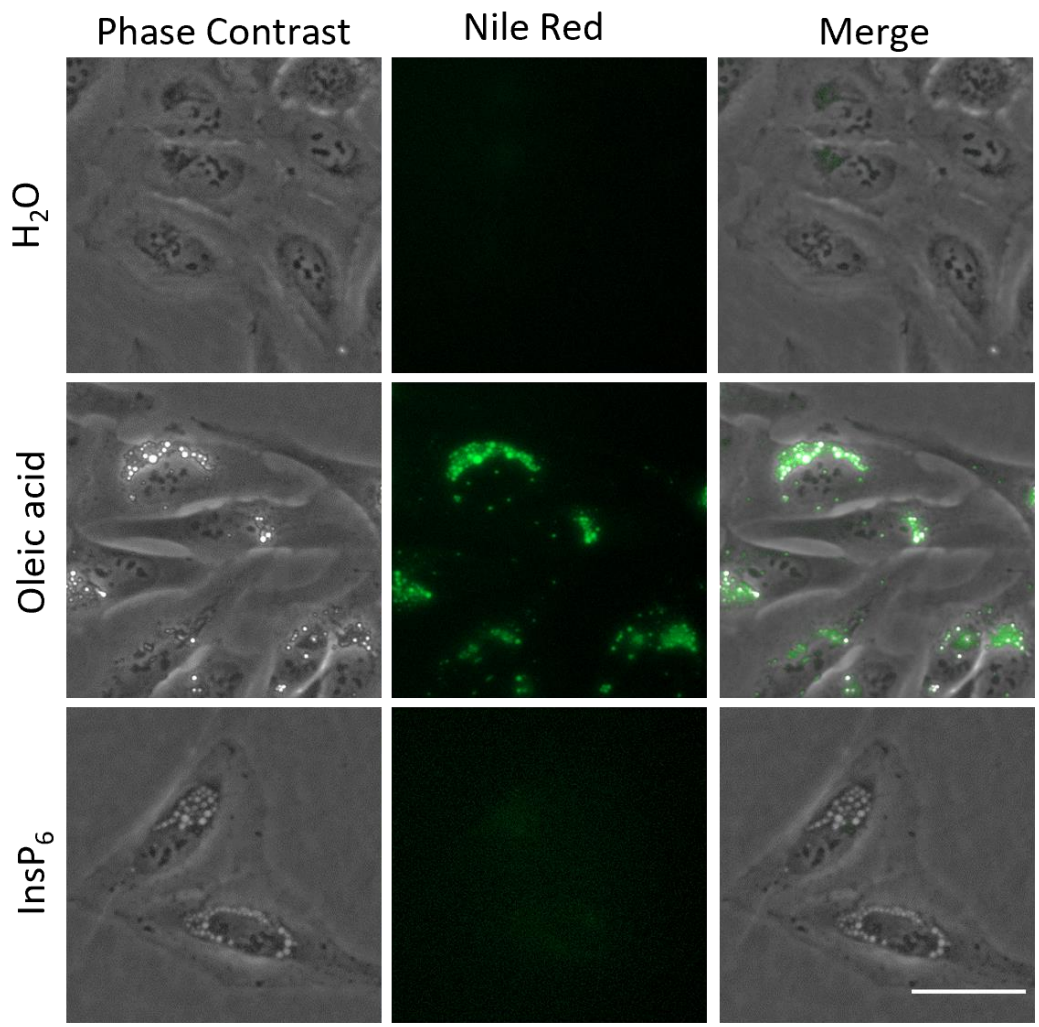

Figure 3.11 $InsP_6$ induced vesicles are not lipophilic. U2-OS cells were treated with either H_2O, 100 µM Oleic acid or 100 µM $InsP_6$ for 24 h. Cells were incubated with 1 µg/mL Nile red for 15 minutes prior to imaging. Cells were imaged by phase contrast and fluorescent microscopy and exposure settings were kept constant throughout. Scale bar = 50 µm.

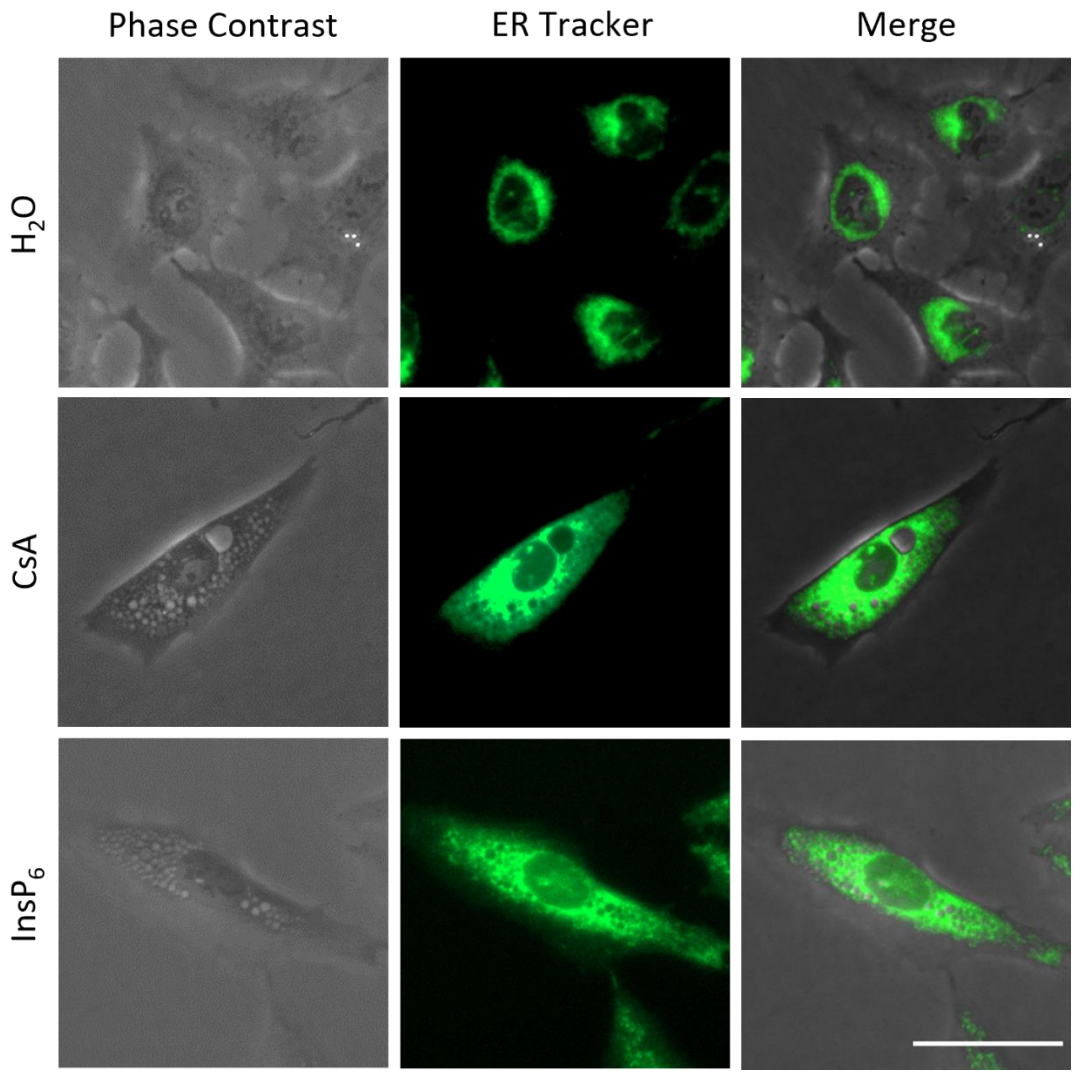

Figure 3.12 $InsP_6$ induced vesicles are localized to the endoplasmic reticulum. U2-OS cells were treated with either H_2O, 30 µM CsA or 100 µM $InsP_6$ for 24 h. Cells were incubated with 1X of ER Cytopainter (ab139481) for 15 min prior to imaging. Cells were imaged by phase contrast and fluorescent microscopy and exposure settings were kept constant throughout. Scale bar = 50 µm.

Chapter 4

General Discussion

IPs are a diverse group of chemically distinct but related compounds. Over the last 50 years a broad range of biological functions have been attributed to individual IPs. Some of these functions have been identified from experiments in vitro where cells have been exposed to IPs (Huang et al., 1997; Irvine & Schell, 2001; Maffucci & Falasca, 2020; Sakamoto et al., 1993; Vucenik et al., 2020). Most IPs, however, have not been studied in vitro as they are difficult to synthesize and are thus unavailable commercially (Best et al., 2010). When I began my research project in the Spring of 2022, previous work in Dr. Mosimann's laboratory had produced and purified many IPs not readily available to other researchers around the world. Conveniently, Dr. Golsteyn's laboratory was already positioned to conduct discovery-based investigations of novel compounds in vitro using human cancer cells. Therefore, we chose to merge the research of both laboratories to investigate the effects of unique IPs on human cancer cells. The goal of this project, then, was to search for and identify novel phenotypic changes in human cancer cells in response to treatment with IPs.

Before testing our unique IPs, we conducted initial screens on the common IP, $InsP_6$. We found that cells treated with $InsP_6$ formed vesicles in their cytoplasm. Despite $InsP_6$ being relatively well characterized, we were unable to find any mention of vesicle formation in any of these reports. Therefore, while not originally the goal of my project, we decided to conduct experiments to characterize further the observed vesicles and their possible mechanism of formation. By fluorescence microscopy, we determined that the vesicles were in the ER. We also noted the appearance of precipitate in the media of cells

treated with $InsP_6$ alongside the vesicle phenotype. The presence of precipitate appeared to correlate with formation of vesicles indicating that the two phenomena may be associated. However, we determined that the physical interaction of the precipitate with cells was not the cause of vesicle formation, nor did the precipitate appear to be depleting the cells of essential cations like calcium and iron, likely constituents of the precipitate.

Finally, the central significance of our investigation came from the finding that some of our unique IPs, two $InsP_5$ isomers, induced the same vesicle phenotype and precipitation as $InsP_6$. This indicates that the induction of vesicles is not specific to $InsP_6$ but that other structurally similar molecules can have the same effect. Additionally, we predict that the ability to induce the vesicle phenotype is limited to higher-phosphorylated IPs, such as $InsP_5$ and $InsP_6$ given that one $InsP_4$ isomer and an isosteric analog of $InsP_6$, $InsS_6$, could not produce the same vesicle phenotype. To summarize, not only did we accomplish the goal of my project by identifying a phenotypic change in response to our unique IPs, but we also discovered that the same phenotypic change was present in $InsP_6$, an already widely studied IP.

4.1 $InsP_6$ induces vesicles in two human cancer cells lines

We observed that treatment with micromolar $InsP_6$ induced vesicles in U2-OS cells. We confirmed that this is a broad cellular effect by showing that a second cell line, HT-29, also acquired vesicles in response to $InsP_6$ treatment. To our knowledge we are the first to report vesicle formation in response to $InsP_6$ treatment in any human cancer cell line. This is interesting given that $InsP_6$ has been tested in a broad range of human cancer cells lines, recently reviewed by Windhorst et al (Brehm & Windhorst, 2019), yet none of these reports mention vesicles formation. For example, $InsP_6$ has been tested at equivalent or higher

concentrations to our experiments in cancer cell lines from breast, hematopoietic, pancreatic, and colon cells, to name a few (Brehm & Windhorst, 2019). Specifically, HT-29 is one of the cell lines already tested with $InsP_6$, however reports from HT-29 cells do not mention vesicle formation and do not include images of their cells post treatment (Saied & Shamsuddin, 1998; Yang & Shamsuddin, 1995). Most reports on $InsP_6$ effects in vitro have not published images of their cells post treatment, and therefore do not offer information as to potential vesicle formation. It is possible that vesicle formation may have occurred in these experiments but simply went unobserved.

4.2 Qualitative characterization of the observed precipitate

Besides vesicles, we also observed the formation of dark precipitate in culture media treated with $InsP_6$. Precipitation was not unexpected given that previous groups have noted its formation in similar model systems where cells were treated with micromolar $InsP_6$ (Windhorst et al., 2013). Physical chemistry studies have also established that divalent cations present in culture media, principally calcium and magnesium, precipitate with $InsP_6$ under conditions similar to culture media (Torres et al., 2005; Vasca et al., 2002; Veiga et al., 2006; Veiga et al., 2009). These experiments were carried out in water where pH and ion concentrations are controlled. It was likely that the precipitate we observed was due to IP-cation interactions. Thus, we sought to confirm that the major constituents of the precipitate were cations.

We determined that calcium was a major component of the precipitate. Of the media components treated with $InsP_6$, only the ones containing calcium ever produced a precipitate in the form of a visual pellet. When calcium was substantially chelated with EGTA prior to $InsP_6$ treatment, no pellet was observed. This indicates that calcium is

necessary for formation of a pellet and confirms previous reports that calcium is the dominant cation present in the $InsP_6$ precipitate in media (Veiga et al., 2006). Interestingly, these reports also state that magnesium is capable of precipitating with micromolar $InsP_6$. However, when we tested the media component without calcium – magnesium being the only stoichiometrically relevant cation in this component – we did not observe a pellet. Therefore, we conclude that magnesium is not present at a concentration sufficient to produce insoluble precipitate, yet it could likely be bound to $InsP_6$ and exist as soluble complexes in solution .

It is possible that that the precipitate contains both calcium and magnesium. Here, Veiga suggests that a good rule of thumb is to expect the relative composition of calcium and magnesium in the precipitate to strongly bias calcium (Veiga et al., 2006). It is likely that the precipitate we observe contains both calcium and magnesium, but that calcium is present at a relatively higher concentration. Besides, magnesium and calcium, the only remaining cations in the salt component of DMEM/F12 are zinc, iron and copper. While all three have an affinity for $InsP_6$ (Torres et al., 2005), and may be present in the precipitate, their trace concentrations (< 2 μM)(Table 1) make them stoichiometrically irrelevant to the formation of $InsP_6$ precipitate.

Additionally, $InsP_6$ was also determined to be a component of the precipitate. At concentrations of 10, 100, and 1000 μM $InsP_6$, at least 50% of the $InsP_6$ initially added appeared in the precipitate 30 minutes later for all concentrations. While this technique does not offer quantitative estimates of the $InsP_6$ present in the precipitate, it does qualitatively confirm that $InsP_6$ is present in the precipitate. The values in Figure 3.3 should not be used to infer solubility limits of the $InsP_6$ in media.

Our determination that calcium and $InsP_6$ are major components of the precipitate agree with the predictions present in the literature (Shears, 2001; Veiga et al., 2006). This conclusion does not rule out the possibility that other cations or biomolecules are also present in the precipitate. For example, one report found that metals present in trace concentrations were able to bind a calcium-$InsP_6$ precipitate thereby becoming insoluble (Wise & Gilburt, 1981). This could be the case for iron, zinc and copper which are known to share high affinity for $InsP_6$ (Torres et al., 2005). Additionally, proteins such as Bovine Serum Albumin (BSA) present in the media have been shown to precipitate with $InsP_6$ under specific conditions (Kaspchak et al., 2019). It could be that the precipitate contains molecules other than cations alone. To understand fully the chemical composition of the precipitate, techniques such as inductively coupled plasma – mass spectroscopy (ICP-MS) or atomic absorption spectroscopy (AAS) could be utilized. Ultraviolet (UV) spectroscopy could also identify the presence of peptides in the precipitate.

4.3 Proximity of the $InsP_6$ precipitate to cells is not necessary for the vesicle phenotype

We next determined that proximity of the visible precipitate to cells was not necessary for the induction of vesicles. Rather our data suggest that $InsP_6$ induces vesicles through a diffusion-based mechanism, where the unique emergent properties of the visible $InsP_6$-calcium precipitate are not necessary for the vesicle phenotype. This is a novel discovery of our research given that we are also the first to report vesicle formation in response to $InsP_6$.

Significantly, the mere presence of $InsP_6$ precipitate creates a confounding variable when investigating vesicle formation. Previous studies report that precipitates in cell culture models can cause biological effects on cells, these effects being dependent on the

emergent properties of the precipitate itself. For example, calcium phosphate precipitate (CCP), widely used to transfect DNA (Kwon & Firestein, 2013), has been shown to induce autophagy as a byproduct of its structural characteristics (Chen et al., 2014; Gao et al., 2008). A hallmark of autophagy is the induction of autophagic vesicles. The CCP interacts with cell surfaces in a way that induces autophagy. Noting the similarity of CCP, both in composition and appearance by light microscopy, to the $InsP_6$ precipitate, we carefully considered the possibility that the vesicle phenotype was dependent on the proximity of the visible $InsP_6$ precipitate to the cells in our model system. To test this, we designed an experiment where the precipitate was localized to a specific regions of cell culture flasks. This allowed us to compare cells in proximity to the precipitate with cells that were only exposed to the precipitate through the diffusion of soluble components. We found that vesicle formation is not dependent on the presence of $InsP_6$-calcium precipitate being adjacent to cells, as vesicles were observed in cells isolated from $InsP_6$-calcium precipitate (Figure 3.4). Additionally, this provokes the hypothesis that the $InsP_6$ precipitate may modify the media in a way that induces vesicle formation in cells. Specifically, the precipitate may deplete the media of a necessary component, whereby the depletion of this component induces the vesicle phenotype.

Here, a distinction between “visible” precipitate and soluble complexes must be made. The resolution limit of conventional light microscopy is ~ 200 nm, making all complexes or precipitates < 200 nm undetectable in our images. IP-metal complexes smaller than 200 nm may have been present in the non-PPT corner but were not detected. Thus, the conclusion above should really be stated as follows: proximity of $InsP_6$ precipitate larger than 200 nm is not necessary for the vesicle phenotype. Throughout the

rest of this thesis, the term “precipitate” will be restricted to the use of the precipitate we observed by light microscopy which we assume to be > 200 nm. IP-metal complexes and precipitates smaller than 200 nm, will be termed soluble complexes. This distinction is important given that Viega and colleagues have identified the existence of these soluble IP-metal complexes. Their reports suggest that in conditions such as those in our experiments, some fraction of $InsP_6$ exists as soluble IP-metal complexes. The effect of these “non-visible”, soluble complexes cannot be ruled out as a potential contributing factor to vesicle formation.

4.4 Removal of the $InsP_6$ precipitate from the media prior to treatment maintains the vesicle phenotype

Having established that the vesicle phenotype is not dependent on the proximity of precipitate with cells but rather a soluble mechanism, we sought to test the hypothesis that the precipitate may be depleting the media of a component essential to the cells. We tested it by removing the precipitate prior to treating the cells, thereby removing any element present in the media. We found that cells exposed to media that had been pre-treated with $InsP_6$, left to precipitate, and had the precipitate removed, showed a similar vesicle phenotype to cells where the $InsP_6$ precipitate was not removed from media exposed to cells. Like the previous experiment in which cells were isolated from precipitate, this observation further rules out the possibility that interactions between the precipitate and cells may be the cause of vesicle formation.

It is possible that the soluble fraction of $InsP_6$ left in the media is responsible for the vesicle phenotype. As stated above, we do not quantitatively understand the fraction of soluble $InsP_6$ remaining in the supernatant following centrifugation. It is also possible that

the technical process of removing precipitate by centrifugation and pipetting of the supernatant back on to cells did not remove all precipitate. While no significant precipitate was observed by light microscopy after the precipitate removal, it may be, as already discussed in the case of the non-PPT corner, that some quantity of $InsP_6$ is left as soluble IP-metal complexes or "non-visible" precipitate in the media, and that this quantity is sufficient to induce vesicles alone. This seems unlikely, however, given that we suspect the soluble concentration of $InsP_6$ left after precipitation to be less than 1 μM (Torres et al., 2005; Veiga et al., 2006), and that this concentration is not capable of inducing vesicle formation in cells (Figure 3.1).

To summarize, the observation that the removal of the $InsP_6$ precipitate prior to treatment maintains the vesicle phenotype leaves us with two possible mechanisms for vesicle formation. First, an essential component of the extracellular media could be trapped in the precipitate and is thereby depleted from the media. This depletion would then be the cause of vesicle formation. Or second, vesicle formation is associated with the soluble fraction of $InsP_6$ left after precipitate removal. In either case, it suffices to say that adding $InsP_6$ to media modifies the media in such a way as to induce vesicle formation.

4.5 Neither calcium nor iron depletion induce vesicles

4.5.1 Calcium depletion by EGTA does not induce vesicles

Depletion of calcium by EGTA did not induce the vesicle phenotype. Given that calcium is a central component of the precipitate, and having established that depletion of some component in the media by the precipitate is a principal hypothesis explaining vesicle formation, we initially thought it plausible that the induction of vesicles is driven by calcium depletion. This prediction is supported in the literature by reports that the

application of micromolar $InsP_6$ in vitro deplete cells of extracellular calcium (Letcher et al., 2008; Shears, 2001). To test whether calcium depletion was the mechanism behind vesicle formation in our experiments we used the specific calcium chelator, EGTA, at concentrations known to deplete the extracellular media of calcium (Milosevic et al., 2006). Cells treated with 1 and 1.5 mM EGTA induced morphologies consistent with disassembled cell-cell contacts resulting from inhibited cadherin function, as previously reported at these EGTA concentrations (Rothen-Rutishauser et al., 2002; Takadera et al., 2010). Since cells did not form vesicles in calcium depleted media, but rather formed a different morphology, the prediction that the vesicles observed $InsP_6$ treated cells are the result of calcium depletion by the precipitate is not supported.

This conclusion does not mean that the soluble calcium concentration in the extracellular media is unaffected by $InsP_6$. While the molar ratio of $InsP_6$ to calcium in our precipitate is unknown, given the complex system and uncharacterized nature of the conditions in which it forms, previously characterized $InsP_6$ precipitates allow us to speculate. All reported divalent metal solids of $InsP_6$ range between 4:1 and 6:1 metal to IP molar ratios, the most common being 5:1 (Bebot-Brigaud et al., 1999; Evans & Martin, 1992; Vasca et al., 2002; Veiga et al., 2006). Consequently, our observed precipitate likely does not exceed a 6:1 calcium to $InsP_6$ molar ratio and the precipitate formed at 100 μM $InsP_6$ in our experiments could remove no more than 600 μM calcium, approximately 50 % of the extracellular calcium pool (Table 3.1). Therefore, while calcium depletion may not be the mechanism of vesicle formation, the $InsP_6$ precipitate could still reduce the soluble calcium pool by 50 % which is likely not sufficient to induce disassembly of cell-cell contacts.

4.2.2 Iron depletion by DFO does not induce vesicles

Other cations present at trace concentrations in the media, and correspondingly small concentrations in the $InsP_6$-precipitate, could also be depleted by precipitate removal. As discussed above, zinc, magnesium, and iron all have affinity for $InsP_6$ (Torres et al., 2005). It is possible that one or several of these cations, though present at concentrations too low to induce precipitation with $InsP_6$ alone (Table 3.2), are incorporated into the $InsP_6$-calcium precipitate. Given that $InsP_6$ has high affinity for iron (Marolt et al., 2020; Odani et al., 2011), especially ferric iron (Nielsen et al., 2013), and reduces iron absorption in vivo and in vitro (Glahn et al., 2002; Hurrell & Egli, 2010; Ma et al., 2011) we asked if iron depletion was the cause of vesicles formation by Deferoxamine (DFO), a known iron chelator. Interestingly, DFO has been reported to induce ER localized vacuoles in cardiomyocytes in vitro (Hoes et al., 2018). However, incubation of DFO at similar concentrations to Hoes et al. with U2-OS cells did not produce the vesicle phenotype. The possibility that iron depletion is the cause of $InsP_6$ vesicle formation is complicated further by the fact that FBS (containing holo-transferrin) is the main source of iron in cell culture media (Young & Garner, 1990). Thus, the concentration of total iron (ferrous and ferric) in any FBS batch may vary, and any chelation effects of $InsP_6$ on iron in the extracellular environment would interplay with transferrin-iron binding. Overall, these results do not support the hypothesis that iron depletion by the $InsP_6$ precipitate is the cause of vesicle formation.

4.6 Characterization of vesicles

Up until this point, our investigation into the cause of vesicle formation has centered on the precipitate as a potential extracellular factor. A second approach is to study

the vesicles directly through fluorescent staining. We found that cells exposed to either $InsP_6$ or CsA show similar vesicles located within the ER, as determined by selective staining of the ER membrane network. Vesicles in the ER can be a sign of various biological effects already known in the literature. In general, vesicles, sometimes referred to as vacuoles in the literature, are formed as cells attempt to manage stress. Two cellular responses known to produce vesicle in the ER are ER stress, also known as the Unfolded Protein Response (UPR) and autophagy (Chino & Mizushima, 2023; Reggiori & Molinari, 2022a). Interestingly, the ER localized vesicles induced by CsA are positive for autophagy markers (Ciechomska et al., 2013). This raises the question, therefore, whether the IP induced vesicles are autophagic as they appear morphologically similar to those induced by CsA. While our fluorescent marker is specific to the ER, it does not offer further information on specific responses such as autophagy or UPR. Further characterization is necessary to determine if either of these cellular responses are indeed involved in the observed vesicle phenotype. Regardless, the fact that we were able to localize the vesicles to the ER is a significant step forward in understanding the vesicle phenotype.

4.7 Formation of precipitate and vesicles is not specific to $InsP_6$

A central complexity in IP research is the phenomenon of redundant effects between certain IPs. Examples in the literature exist where $InsP_5$ and $InsP_6$ have redundant effects or $InsP_3$ and $InsP_4$ induce similar signal cascades (Irvine & Schell, 2001; Shears, 2001). Therefore, we asked if the vesicle and precipitation we observed after $InsP_6$ treatment extends to other IPs and structurally related compounds.

4.7.1 $InsS_6$ neither forms precipitate in media nor induces vesicles in cells

We asked if $InsS_6$, a structural analog of $InsP_6$, could also induce the vesicle phenotype. $InsS_6$ is a synthetic compound where the phosphates of $InsP_6$ are replaced with sulphates. It that has been reported to interact with proteins similarly to $InsP_6$ and promote similar effects (Larsson et al., 1997; Ullah & Sethumadhavan, 1998). For this reason, Shears recommends that any observed $InsP_6$ effect in vitro, be controlled with $InsS_6$ to clarify the specificity of $InsP_6$ (Shears, 2001). In our results, however, $InsS_6$ was unable to form precipitate in media or induce vesicles formation in cells at all concentrations tested. Therefore, we conclude that structural components of $InsP_6$, likely the phosphate groups, are necessary for the observed vesicle phenotype, and that isosteric substitution of those phosphates with sulphates removes the phenotype.

4.7.2 Ins(1,2,4,5,6)P_5 and Ins(2,3,4,5,6)P_5 form precipitate in media and induce the vesicle phenotype whereas Ins(1,2,3,4)P_4 does neither

A central significance of our results is that both Ins(1,2,4,5,6)P_5 and Ins(2,3,4,5,6)P_5 produce the same precipitate and vesicle phenotype as $InsP_6$ in our cell-based assays. As in the case of $InsP_6$, precipitate formation in media by $InsP_5$ was not unexpected. While specific solubility limits for the $InsP_5$ isomers we tested have not been reported in media, it is safe to assume from the literature that at 100 μM of either $InsP_5$ isomer, some concentration will form precipitate. For example, barring stereospecific exceptions, $InsP_5$ and $InsP_6$ have been shown to precipitate similarly in calcium and magnesium solutions (Veiga et al., 2006; Veiga et al., 2009). Although these reports suggest that $InsP_5$ isomers are, in general, slightly more soluble than $InsP_6$.

Interestingly, the presence of precipitate appeared to correlate with vesicle formation. Cells treated with 100 μM of both $InsP_5$ isomers, a concentration where clear precipitate was observed throughout the well, induced vesicles in over 90 % of cells observed (Figure 3.8). Whereas cells treated with lower concentrations of both $InsP_5$ isomers showed neither vesicles nor precipitate in media. A similar correlation was previously observed in the $InsP_6$ experiments. Having already determined, in the case of $InsP_6$, that vesicle formation is not dependent on the presence of precipitate, we asked if the same was true for $InsP_5$. We found that removal of the Ins(2,3,4,5,6)P_5 precipitate prior to treatment with cells caused vesicle formation, just as in the case of $InsP_6$.

Additionally, Ins(1,2,3,4)P_4 failed to form precipitate or induce vesicles at all concentrations tested (Figure 3.8). Given that we suspect the precipitation of IPs in media to be driven by the interaction of cations with the negative phosphoryl groups of IPs, it is not surprising that a lower phosphorylated IP was unable to precipitate in media. Although stereospecificity of the phosphoryl locations is a factor, in general, literature assumes that the less phosphoryl groups attached to an IP, the less strongly it interacts and precipitates with cations (Lonnerdal et al., 1989; Luttrell, 1993). It is also worth noting that the correlation of vesicle formation and precipitation continues in this experiment. However, taken alongside the $InsP_6$ and $InsP_5$ experiments, it agrees with the trend that vesicle formation appears to be correlated with precipitation.

Importantly, instances where IPs have overlapping biological effects have already been identified in the literature. For example, upon microinjection with $InsP_5$ and $InsP_6$, Xenopus oocytes showed desensitization of heterologously expressed substance P receptors (Sasakawa et al., 1994; Shears, 2001; Vallejo et al., 1987). Interestingly, the $InsP_3$

and $InsP_4$ isomers were also microinjected, but showed no effect. Additionally, $InsP_5$ and $InsP_6$ have both been reported to influence cardiovascular function upon infusion into rat brain stems (Sasakawa et al., 1994; Shears, 2001; Vallejo et al., 1987). This observation was later explained by the fact that $InsP_5$ and $InsP_6$ both chelate calcium (Shears, 2001). The effect on the local calcium pool is now considered to be the cause of altered cardiovascular function. In these examples, the structural similarity of $InsP_5$ to $InsP_6$ have been shown to account for the similarity in function. Therefore, it is reasonable to predict that the structural similarity of Ins(1,2,4,5,6)P_5 and Ins(2,3,4,5,6)P_5 with $InsP_6$ explain the similarity in their induced vesicle phenotype. Likewise, it is reasonable to predict that the lack of a vesicle phenotype in cells treated with Ins(1,2,3,4)P_4 is due to its greater dissimilarity in structure from $InsP_6$. These results lead to the conclusion that structural components of IPs (degree of phosphorylation) correlate with precipitation in media and the formation of vesicles in cells.

4.8 Conclusion

In this thesis we have identified a new phenotype not previously reported in the literature. We found that $InsP_6$ induces vesicles in the ER of two human cancer cells lines, U2-OS and HT-29. Significantly, we also found that Ins(1,2,4,5,6)P_5 and Ins(2,3,4,5,6)P_5 induce the same phenotype, whereas Ins(1,2,3,4)P_4 was unable to induce the vesicle phenotype. Therefore, we have met the first objective of this thesis, which was to search for and identify phenotypic changes in human cancer cells upon treatment with both common and unique myo-inositol phosphates.

Importantly, we noted the presence of precipitate in culture media following treatment with $InsP_6$ and both $InsP_5$ isomers, which we were able to dissociate from the

formation of vesicles in cells. We determined that the precipitate contained calcium and $InsP_6$ thereby meeting our second objective to analyze the precipitate's composition. This observation led to a second mechanistic hypothesis that vesicles were induced through extracellular cation depletion by the precipitate. We could not provide evidence to support this hypothesis, however, given that neither EGTA nor DFO induced vesicles. In summary, we determined that both $InsP_5$ and $InsP_6$ precipitates correlate with vesicle formation, but that they are not necessary for the vesicle phenotype, and do not induce vesicles through calcium or iron depletion. The determination that the precipitate is not necessary for the vesicle phenotype answered our third objective, which was to characterize the role of the precipitate in the formation of vesicles.

We also predict that the specificity of the vesicle phenotype is limited to higher-phosphorylated IPs. We predict this for two reasons. First, one $InsP_4$ isomer was unable to precipitate or induce the vesicle phenotype, and second, the structural analog of $InsP_6$, $InsS_6$, also was unable to precipitate or induce vesicle formation. This suggests that the structural characteristics of phosphate groups are necessary for the vesicle phenotype. Overall, these two results partially define the structural characteristics necessary to induce the vesicle phenotype in cells.

To our knowledge, we are the first to report IP-mediated vesicle formation within the ER in any human cell line. Therefore, the novel discovery that $InsP_6$ induces vesicle formation in the ER of human cancer cells offers new insights relevant to mechanistic discussion behind exogenous $InsP_6$ effects, especially those already present in the literature.

4.9 Future Directions

4.9.1 Potential intracellular effects of *myo*-inositol phosphates

In our discussion we left open the possibility that some soluble fraction of both $InsP_5$ and $InsP_6$ present in our experiments could account for the formation of vesicles. As part of the interpretation of our results, we came across several studies relevant to this possible mechanism. While IPs are generally considered unable to enter cells by diffusion across the plasma membrane due to their high charge density, several reports have indicated that exogenous $InsP_6$ and some $InsP_5$s do enter tissue culture cells in vitro (Ferry et al., 2002; Helmis et al., 2013; Riley et al., 2014; Windhorst et al., 2013). Most recently, Windhorst and colleagues have shown results indicating $InsP_6$ is taken up by cells via IP-metal complexes. They conclude that the positive charge density of the bound cation interacts with the negatively charged glycocalyx of cell's extracellular matrix ECM, localizing the IP to the membrane where it can be taken up by endocytosis. It is possible that $InsP_5$ and $InsP_6$ internalized via this mechanism are responsible for the vesicle phenotype. This hypothesis could form the basis of future research.

4.9.2 Analysis of the precipitate

The alternative hypothesis we suggested is that the precipitate may deplete the media of an essential component, whereby depletion of this component induces vesicles in cells. Although we challenged the idea that this component was calcium or iron, it may be that the component is yet to be identified. Here, a full analysis of the precipitate would prove valuable. ICP-MS could provide a full chemical analysis of all cations present in the precipitate. Possible metal candidates are zinc, copper, and magnesium, given the media conditions (Table 3.1). While less likely, possible non-metal components include proteins and organic molecules, which could also be identified by mass spectroscopy. A full

understanding of the chemical composition of the precipitate could offer insights into this discussion.

REFERENCES

Anderson, L., & Wolter, K. E. (1966). Cyclitols in plants - biochemistry and physiology. *Annual Review of Plant Physiology*, *17*, 209–222.

Barrientos, L. G., & Murthy, P. P. (1996). Conformational studies of myo-inositol phosphates. *Carbohydrate Research*, *296*, 39-54.

Bebot-Brigaud, A., Dange, C., Fauconnier, N., & Gérard, C. (1999). P NMR, potentiometric and spectrophotometric studies of phytic acid ionization and complexation properties toward Co, Ni, Cu, Zn and Cd. *Journal of Inorganic Biochemistry*, *75*, 71-78.

Berridge, M. J., & Irvine, R. F. (1989). Inositol phosphates and cell signalling. *Nature*, *341*, 197-205.

Best, M. D., Zhang, H., & Prestwich, G. D. (2010). Inositol polyphosphates, diphosphoinositol polyphosphates and phosphatidylinositol polyphosphate lipids: structure, synthesis, and development of probes for studying biological activity. *Natural Product Reports*, *27*, 1403-1430.

Bizzarri, M., Dinicola, S., Bevilacqua, A., & Cucina, A. (2016). Broad spectrum anticancer activity of myo-inositol and inositol hexakisphosphate. *International Journal of Endocrinology*, *2016*, e5616807.

Bohn, L., Meyer, A. S., & Rasmussen, S. K. (2008). Phytate: impact on environment and human nutrition. A challenge for molecular breeding. *Journal of Zhejiang University Science B*, *9*, 165-191.

Borgese, T. A., & Nagel, R. L. (1977). Differential effects of 2,3-dpg, atp and inositol pentaphosphate (Ip5) on oxygen equilibria of duck embryonic, fetal and adult hemoglobins. *Comparative Biochemistry and Physiology a-Molecular & Integrative Physiology*, *56*, 539-543.

Brasaemle, D. L., Barber, T., Kimmel, A. R., & Londos, C. (1997). Post-translational regulation of perilipin expression. Stabilization by stored intracellular neutral lipids. *Journal of Biological Chemistry*, *272*, 9378-9387.

Brehm, M. A., & Windhorst, S. (2019). New options of cancer treatment employing InsP(6). *Biochemal Pharmacology*, *163*, 206-214.

Bruder, L. M., Gruninger, R. J., Cleland, C. P., & Mosimann, S. C. (2017). Bacterial PhyA protein-tyrosine phosphatase-like myo-inositol phosphatases in complex with the Ins(1,3,4,5)P(4) and Ins(1,4,5)P(3) second messengers. *Journal of Biological Chemistry*, *292*, 17302-17311.

Campbell, S., Fisher, R. J., Towler, E. M., Fox, S., Issaq, H. J., Wolfe, T., Phillips, L. R., & Rein, A. (2001). Modulation of HIV-like particle assembly in vitro by inositol phosphates. *Proceedings of the National Academy of Science of the United States of America*, *98*, 10875-10879.

Cecconi, O., Nelson, R. M., Roberts, W. G., Hanasaki, K., Mannori, G., Schultz, C., Ulich, T. R., Aruffo, A., & Bevilacqua, M. P. (1994). Inositol polyanions. Noncarbohydrate inhibitors of L- and P-selectin that block inflammation. *Journal of Biological Chemistry*, *269*, 15060-15066.

Chen, X., Khambu, B., Zhang, H., Gao, W., Li, M., Chen, X., Yoshimori, T., & Yin, X. M. (2014). Autophagy induced by calcium phosphate precipitates targets damaged endosomes. *Journal of Biological Chemistry*, *289*, 11162-11174.

Chino, H., & Mizushima, N. (2023). ER-phagy: quality and quantity control of the endoplasmic reticulum by autophagy. *Cold Spring Harbor Perspectives in Biology*, *15*, e041256.

Ciechomska, I. A., Gabrusiewicz, K., Szczepankiewicz, A. A., & Kaminska, B. (2013). Endoplasmic reticulum stress triggers autophagy in malignant glioma cells undergoing cyclosporine a-induced cell death. *Oncogene*, *32*, 1518-1529.

Costello, A. J., Glonek, T., & Myers, T. C. (1976). 31P nuclear magnetic resonance-pH titrations of myo-inositol hexaphosphate. *Carbohydrate Research*, *46*, 159-171.

Cui, L., Li, H., Xi, Y., Hu, Q., Liu, H., Fan, J., Xiang, Y., Zhang, X., Shui, W., & Lai, Y. (2022). Vesicle trafficking and vesicle fusion: mechanisms, biological functions, and their implications for potential disease therapy. *Molecular Medicine*, *3*, e29.

Dilworth, L., Stennett, D., & Omoruyi, F. (2023). Cellular and molecular activities of IP6 in disease prevention and therapy. *Biomolecules*, *13*, e972.

Evans, W. J., & Martin, C. J. (1992). Interactions of inositol hexaphosphate with Pb(Ii) and Be(Ii) - a calorimetric study. *Journal of Inorganic Biochemistry*, *45*, 105-113.

Ferry, S., Matsuda, M., Yoshida, H., & Hirata, M. (2002). Inositol hexakisphosphate blocks tumor cell growth by activating apoptotic machinery as well as by inhibiting the Akt/NFkappaB-mediated cell survival pathway. *Carcinogenesis*, *23*, 2031-2041.

Fu, M., Song, Y., Wen, Z., Lu, X., & Cui, L. (2016). Inositol hexaphosphate and inositol inhibit colorectal cancer metastasis to the liver in BALB/c mice. *Nutrients*, *8*, e286.

Gao, W., Ding, W. X., Stolz, D. B., & Yin, X. M. (2008). Induction of macroautophagy by exogenously introduced calcium. *Autophagy*, *4*, 754-761.

Glahn, R. P., Wortley, G. M., South, P. K., & Miller, D. D. (2002). Inhibition of iron uptake by phytic acid, tannic acid, and $ZnCl_2$: studies using an in vitro digestion/Caco-2 cell model. *Journal of Agricultural and Food Chemistry*, *50*, 390-395.

Grases, F., Garcia-Gonzalez, R., Torres, J. J., & Llobera, A. (1998). Effects of phytic acid on renal stone formation in rats. *Scandinavian Journal of Urology and Nephrology*, *32*, 261-265.

Greenspan, P., Mayer, E. P., & Fowler, S. D. (1985). Nile red: a selective fluorescent stain for intracellular lipid droplets. *Journal of Cell Biology*, *100*, 965-973.

Hanakahi, L. A., Bartlet-Jones, M., Chappell, C., Pappin, D., & West, S. C. (2000). Binding of inositol phosphate to DNA-PK and stimulation of double-strand break repair. *Cell*, *102*, 721-729.

Hartig, T. (1855). Ueber das Klebermehl. *Flora oder Botanische Zeitung*, *881*.

Hawkins, P. T., Poyner, D. R., Jackson, T. R., Letcher, A. J., Lander, D. A., & Irvine, R. F. (1993). Inhibition of iron-catalysed hydroxyl radical formation by inositol polyphosphates: a possible physiological function for myo-inositol hexakisphosphate. *Biochemal Journal*, *294*, 929-934.

Helmis, C., Blechner, C., Lin, H., Schweizer, M., Mayr, G. W., Nielsen, P., & Windhorst, S. (2013). Malignant H1299 tumour cells preferentially internalize iron-bound inositol hexakisphosphate. *Bioscience Reports*, *33*, e00075.

Heslop, J. P., Irvine, R. F., Tashjian, A. H., & Berridge, M. J. (1985). Inositol tetrakisphosphate and pentakisphosphate in Gh4 cells. *Journal of Experimental Biology*, *119*, 395-401.

Hoes, M. F., Beverborg, N. G., Kijlstra, J. D., Kuipers, J., Swinkels, D. W., Giepmans, B. N. G., Rodenburg, R. J., Van Veldhuisen, D. J., De Boer, R. A., & Van der Meer, P. (2018). Iron deficiency impairs contractility of human cardiomyocytes through decreased mitochondrial function. *European Journal of Heart Failure*, *20*, 627-627.

Huang, C., Ma, W. Y., Hecht, S. S., & Dong, Z. (1997). Inositol hexaphosphate inhibits cell transformation and activator protein 1 activation by targeting phosphatidylinositol-3' kinase. *Cancer Research*, *57*, 2873-2878.

Hurrell, R., & Egli, I. (2010). Iron bioavailability and dietary reference values. *American Journal of Clinical Nutrition*, *91*, 1461-1467.

Irvine, R. F., & Schell, M. J. (2001). Back in the water: the return of the inositol phosphates. *Nature Reviews Molecular Cell Biology*, *2*, 327-338.

Isbrandt, L. R., & Oertel, R. P. (1980). Conformational states of myoinositol hexakisphosphate in aqueous-solution - a C-13 nmr, P-31 nmr, and raman-spectroscopic investigation. *Journal of the American Chemical Society*, *102*, 3144-3148.

Kaspchak, E., Goedert, A. C., Igarashi-Mafra, L., & Mafra, M. R. (2019). Effect of divalent cations on bovine serum albumin (BSA) and tannic acid interaction and its influence on turbidity and in vitro protein digestibility. *International Journal of Biological Macromolecules*, *136*, 486-492.

Komander, D., Fairservice, A., Deak, M., Kular, G. S., Prescott, A. R., Downes, C. P., Safrany, S. T., Alessi, D. R., & van Aalten, D. M. F. (2004). Structural insights into the regulation of PDK1 by phosphoinositides and inositol phosphates. *EMBO Journal*, *23*, 3918-3928.

Kwon, M., & Firestein, B. L. (2013). DNA transfection: calcium phosphate method. *Methods in Molecular Biology*, *1018*, 107-110.

Larsson, O., Barker, C. J., Sjoholm, A., Carlqvist, H., Michell, R. H., Bertorello, A., Nilsson, T., Honkanen, R. E., Mayr, G. W., Zwiller, J., & Berggren, P. O. (1997). Inhibition of phosphatases and increased Ca2+ channel activity by inositol hexakisphosphate. *Science*, *278*, 471-474.

Lee, J., Homma, T., Kurahashi, T., Kang, E. S., & Fujii, J. (2015). Oxidative stress triggers lipid droplet accumulation in primary cultured hepatocytes by activating fatty acid synthesis. *Biochemal and Biophysical Research Communications*, *464*, 229-235.

Letcher, A. J., Schell, M. J., & Irvine, R. F. (2008). Do mammals make all their own inositol hexakisphosphate? *Biochemical Journal*, *416*, 263-270.

Liu, G., Song, Y., Cui, L., Wen, Z., & Lu, X. (2015). Inositol hexaphosphate suppresses growth and induces apoptosis in HT-29 colorectal cancer cells in culture: PI3K/Akt pathway as a potential target. *International Journal of Clinical and Experimental Pathology*, *8*, 1402-1410.

Liu, Y. J., & Wang, C. (2023). A review of the regulatory mechanisms of extracellular vesicles-mediated intercellular communication. *Cell Communication and Signalling*, *21*, e77.

Loewus, F. A., & Murthy, P. P. N. (2000). Myo-inositol metabolism in plants. *Plant Science*, *150*, 1-19.

Lonnerdal, B., Sandberg, A. S., Sandstrom, B., & Kunz, C. (1989). Inhibitory effects of phytic acid and other inositol phosphates on zinc and calcium absorption in suckling rats. *Journal of Nutrition*, *119*, 211-214.

Luttrell, B. M. (1993). The biological relevance of the binding of calcium-Ions by inositol phosphates. *Journal of Biological Chemistry*, *268*, 1521-1524.

Luttrell, B. M. (1994). Cellular actions of inositol phosphates and other natural calcium and magnesium chelators. *Cell Signalling*, *6*, 355-362.

Ma, Q., Kim, E. Y., Lindsay, E. A., & Han, O. (2011). Bioactive dietary polyphenols inhibit heme iron absorption in a dose-dependent manner in human intestinal Caco-2 cells. *Journal of Food Science*, *76*, 143-150.

Macbeth, M. R., Schubert, H. L., VanDemark, A. P., Lingam, A. T., Hill, C. P., & Bass, B. L. (2005). Inositol hexakisphosphate is bound in the ADAR2 core and required for RNA editing. *Science*, *309*, 1534-1539.

Maffucci, T., & Falasca, M. (2020). Signalling properties of inositol polyphosphates. *Molecules*, *25*, e5281.

Majerus, P. W., Zou, J., Marjanovic, J., Kisseleva, M. V., & Wilson, M. P. (2008). The role of inositol signaling in the control of apoptosis. *Advances in Enzyme Regulation*, *48*, 10-17.

Marolt, G., Gricar, E., Pihlar, B., & Kolar, M. (2020). Complex formation of phytic acid with selected monovalent and divalent metals. *Frontiers in Chemistry*, *8*, e582746.

Michell, R. H. (2008a). Inositol derivatives: evolution and functions. *Nature Reviews: Molecular Cell Biology*, *9*, 151-161.

Michell, R. H. (2008b). Inositol derivatives: evolution and functions. *Nature Reviews Molecular Cell Biology*, *9*, 151-161.

Milosevic, J., Juch, F., Storch, A., & Schwarz, J. (2006). Low extracellular calcium is sufficient for survival and proliferation of murine mesencephalic neural precursor cells. *Cell and Tissue Research*, *324*, 377-384.

Minihane, A. M., & Rimbach, G. (2002). Iron absorption and the iron binding and anti-oxidant properties of phytic acid. *International Journal of Food Science and Technology*, *37*, 741-748.

Mondal, A., Ashiq, K. A., Phulpagar, P., Singh, D. K., & Shiras, A. (2019). Effective visualization and easy tracking of extracellular vesicles in glioma cells. *Biological Procedures Online*, *21*, e4.

Murthy, P. P. (2006). Structure and nomenclature of inositol phosphates, phosphoinositides, and glycosylphosphatidylinositols. *Subcellular Biochemistry*, *39*, 1-19.

Nielsen, A. V., Tetens, I., & Meyer, A. S. (2013). Potential of phytase-mediated iron release from cereal-based foods: a quantitative view. *Nutrients*, *5*, 3074-3098.

Odani, A., Jastrzab, R., & Lomozik, L. (2011). Equilibrium study on the interaction of phytic acid with polyamines and metal ions. *Metallomics*, *3*, 735-743.

Odom, A. R., Stahlberg, A., Wente, S. R., & York, J. D. (2000). A role for nuclear inositol 1,4,5-trisphosphate kinase in transcriptional control. *Science*, *287*, 2026-2029.

Parkar, N. S., Akpa, B. S., Nitsche, L. C., Wedgewood, L. E., Place, A. T., Sverdlov, M. S., Chaga, O., & Minshall, R. D. (2009). Vesicle formation and endocytosis: function, machinery, mechanisms, and modeling. *Antioxidants and Redox Signaling*, *11*, 1301-1312.

Piccolo, E., Vignati, S., Maffucci, T., Innominato, P. F., Riley, A. M., Potter, B. V., Pandolfi, P. P., Broggini, M., Iacobelli, S., Innocenti, P., & Falasca, M. (2004). Inositol pentakisphosphate promotes apoptosis through the PI 3-K/Akt pathway. *Oncogene*, *23*, 1754-1765.

Pires, S. M. G., Reis, R. S., Cardoso, S. M., Pezzani, R., Paredes-Osses, E., Seilkhan, A., Ydyrys, A., Martorell, M., Gürer, E. S., Setzer, W. N., Razis, A. F. A., Modu, B., Calina, D., & Sharifi-Rad, J. (2023). Phytates as a natural source for health promotion: A critical evaluation of clinical trials. *Frontiers in Chemistry*, *11*, e1174109.

Potter, B. V. L., & Lampe, D. (1995). Chemistry of inositol lipid-mediated cellular signaling. *Angewandte Chemie-International Edition*, *34*, 1933-1972.

Pujol, A., Sanchis, P., Grases, F., & Masmiquel, L. (2023). Phytate intake, health and disease: "let thy food be thy medicine and medicine be thy food". *Antioxidants (Basel)*, *12*, e146.

Quignard, J. F., Rakotoarisoa, L., Mironneau, J., & Mironneau, C. (2003). Stimulation of L-type Ca^{2+} channels by inositol pentakis- and hexakisphosphates in rat vascular smooth muscle cells. *The Journal of Physiology*, *549*, 729-737.

Raeymaekers, L., & Larivière, E. (2011). Vesicularization of the endoplasmic reticulum is a fast response to plasma membrane injury. *Biochemical and Biophysical Research Communications*, *414*, 246-251.

Ram, B. M., & Ramakrishna, G. (2014). Endoplasmic reticulum vacuolation and unfolded protein response leading to paraptosis like cell death in cyclosporine A treated cancer cervix cells is mediated by cyclophilin B inhibition. *Biochimica et Biophysica Acta*, *1843*, 2497-2512.

Reggiori, F., & Molinari, M. (2022a). ER-phagy: mechanisms, regulation, and diseases connected to the lysosomal clearance of the endoplasmic reticulum. *Physiological Reviews*, *102*, 1393-1448.

Reggiori, F., & Molinari, M. (2022b). ER-phagy: mechanisms, regulation, and diseases connected to the lysosomal clearance of the endoplasmic reticulum. *Physiology Reviews*, *102*, 1393-1448.

Riley, A. M., Windhorst, S., Lin, H. Y., & Potter, B. V. (2014). Cellular internalisation of an inositol phosphate visualised by using fluorescent InsP5. *ChemBioChem*, *15*, 57-67.

Rizvi, I., Riggs, D. R., Jackson, B. J., Ng, A., Cunningham, C., & McFadden, D. W. (2006). Inositol hexaphosphate (IP6) inhibits cellular proliferation in melanoma. *Journal of Surgical Research*, *133*, 3-6.

Rothen-Rutishauser, B., Riesen, F. K., Braun, A., Gunthert, M., & Wunderli-Allenspach, H. (2002). Dynamics of tight and adherens junctions under EGTA treatment. *Journal of Membrane Biology*, *188*, 151-162.

Saied, I. T., & Shamsuddin, A. M. (1998). Up-regulation of the tumor suppressor gene p53 and WAF1 gene expression by IP6 in HT-29 human colon carcinoma cell line. *Anticancer Research*, *18*, 1479-1484.

Sakamoto, K., Venkatraman, G., & Shamsuddin, A. M. (1993). Growth inhibition and differentiation of HT-29 cells in vitro by inositol hexaphosphate (phytic acid). *Carcinogenesis*, *14*, 1815-1819.

Sasakawa, N., Ferguson, J. E., Sharif, M., & Hanley, M. R. (1994). Attenuation of agonist-induced desensitization of the rat substance-p receptor by microinjection

of inositol pentakisphosphate and hexakisphosphate in xenopus-laevis oocytes. *Molecular Pharmacology*, *46*, 380-385.

Schlemmer, U., Frolich, W., Prieto, R. M., & Grases, F. (2009). Phytate in foods and significance for humans: food sources, intake, processing, bioavailability, protective role and analysis. *Molecular Nutrition and Food Research*, *53*, 330-375.

Schrader, M., Kamoshita, M., & Islinger, M. (2020). Organelle interplay-peroxisome interactions in health and disease. *Journal of Inherited Metabolic Disease*, *43*, 71-89.

Shamsuddin, A. M., Vucenik, I., & Cole, K. E. (1997). IP6: a novel anti-cancer agent. *Life Sciences*, *61*, 343-354.

Shears, S. B. (2001). Assessing the omnipotence of inositol hexakisphosphate. *Cell Signalling*, *13*, 151-158.

Shears, S. B., Ganapathi, S. B., Gokhale, N. A., Schenk, T. M., Wang, H., Weaver, J. D., Zaremba, A., & Zhou, Y. (2012). Defining signal transduction by inositol phosphates. *Subcellular Biochemistry*, *59*, 389-412.

Shen, X., Xiao, H., Ranallo, R., Wu, W. H., & Wu, C. (2003). Modulation of ATP-dependent chromatin-remodeling complexes by inositol polyphosphates. *Science*, *299*, 112-114.

Skoglund, E., Nasi, M., & Sandberg, A. S. (1998). Phytate hydrolysis in pigs fed a barley-rapeseed meal diet treated with Aspergillus niger phytase or steeped with whey. *Canadian Journal of Animal Science*, *78*, 175-180.

Smith, A. W., Poyner, D. R., Hughes, H. K., & Lambert, P. A. (1994). Siderophore activity of myoinositol hexakisphosphate in pseudomonas-aeruginosa. *Journal of Bacteriology*, *176*, 3455-3459.

Steger, D. J., Haswell, E. S., Miller, A. L., Wente, S. R., & O'Shea, E. K. (2003). Regulation of chromatin remodeling by inositol polyphosphates. *Science*, *299*, 114-116.

Sun, M. K., Wahlestedt, C., & Reis, D. J. (1992). Inositol hexakisphosphate excites rat medullary sympathoexcitatory neurons in vivo. *European Journal of Pharmacology*, *215*, 9-16.

Takadera, T., Ohtsuka, M., & Aoki, H. (2010). Chelation of extracellular calcium-induced cell death was prevented by glycogen synthase kinase-3 inhibitors in PC12 cells. *Cellular and Molecular Neurobiology*, *30*, 193-198.

Tan, X., Calderon-Villalobos, L. I. A., Sharon, M., Zheng, C. X., Robinson, C. V., Estelle, M., & Zheng, N. (2007). Mechanism of auxin perception by the TIR1 ubiquitin ligase. *Nature*, *446*, 640-645.

ThermoFisher. (2024). *Media formulation 11320 - DMEM/F-12*. Retrieved June 18, 2024 from https://www.thermofisher.com/ca/en/home/technical-resources/media-formulation.55.html

Torres, J., Dominguez, S., Cerda, M. F., Obal, G., Mederos, A., Irvine, R. F., Diaz, A., & Kremer, C. (2005). Solution behaviour of myo-inositol hexakisphosphate in the presence of multivalent cations. Prediction of a neutral pentamagnesium species under cytosolic/nuclear conditions. *Journal of Inorganic Biochemistry*, *99*, 828-840.

Tuescher, J. M., Beck, C. R., Spencer, L., Yeremy, B., Shi, Y., Andersen, R. J., & Golsteyn, R. M. (2021). Extracts prepared from a canadian toxic plant induce light-dependent perinuclear vacuoles in human cells. *Toxins*, *13*, 138-153.

Ullah, A. H. J., & Sethumadhavan, K. (1998). Myo-inositol hexasulfate is a potent inhibitor of phytase. *Biochemical and Biophysical Research Communications*, *251*, 260-263.

Urbano, G., Lopez-Jurado, M., Aranda, P., Vidal-Valverde, C., Tenorio, E., & Porres, J. (2000). The role of phytic acid in legumes: antinutrient or beneficial function? *Journal of Physiology and Biochemistry*, *56*, 283-294.

Vajanaphanich, M., Schultz, C., Rudolf, M. T., Wasserman, M., Enyedi, P., Craxton, A., Shears, S. B., Tsien, R. Y., Barrett, K. E., & Traynor-Kaplan, A. (1994). Long-term uncoupling of chloride secretion from intracellular calcium levels by Ins(3,4,5,6)P4. *Nature*, *371*, 711-714.

Vallejo, M., Jackson, T., Lightman, S., & Hanley, M. R. (1987). Occurrence and extracellular actions of inositol pentakis- and hexakisphosphate in mammalian brain. *Nature*, *330*, 656-658.

Vasca, E., Materazzi, S., Caruso, T., Milano, O., Fontanella, C., & Manfredi, C. (2002). Complex formation between phytic acid and divalent metal ions: a solution equilibria and solid state investigation. *Analytical and Bioanalytical Chemistry*, *374*, 173-178.

Veiga, N., Torres, J., Dominguez, S., Mederos, A., Irvine, R. F., Diaz, A., & Kremer, C. (2006). The behaviour of myo-inositol hexakisphosphate in the presence of magnesium(II) and calcium(II): protein-free soluble InsP6 is limited to 49 microM under cytosolic/nuclear conditions. *Journal of Inorganic Biochemistry*, *100*, 1800-1810.

Veiga, N., Torres, J., Godage, H. Y., Riley, A. M., Dominguez, S., Potter, B. V., Diaz, A., & Kremer, C. (2009). The behaviour of inositol 1,3,4,5,6-pentakisphosphate in the presence of the major biological metal cations. *Journal of Biological Inorganic Chemistry*, *14*, 1001-1013.

Vucenik, I. (2019). Anticancer properties of inositol hexaphosphate and inositol: an overview. *Journal of Nutritional Science and Vitaminology (Tokyo)*, *65*, S18-S22.

Vucenik, I., Druzijanic, A., & Druzijanic, N. (2020). Inositol hexaphosphate (IP6) and colon cancer: from concepts and first experiments to clinical application. *Molecules*, *25*, e5931.

Vucenik, I., & Shamsuddin, A. M. (1994). [H-3] Inositol hexaphosphate (phytic acid) is rapidly absorbed and metabolized by murine and human-malignant cells in-vitro. *Journal of Nutrition*, *124*, 861-868.

Weiskirchen, S., Schroder, S. K., Buhl, E. M., & Weiskirchen, R. (2023). A beginner's guide to cell culture: practical advice for preventing needless problems. *Cells*, *12*, e682.

Windhorst, S., Lin, H. Y., Blechner, C., Fanick, W., Brandt, L., Brehm, M. A., & Mayr, G. W. (2013). Tumour cells can employ extracellular Ins(1,2,3,4,5,6)

and multiple inositol-polyphosphate phosphatase 1 (MINPP1) dephosphorylation to improve their proliferation. *Biochemical Journal*, *450*, 115-125.

Wise, A., & Gilburt, D. J. (1981). Binding of cadmium and lead to the calcium-phytate complex in vitro. *Toxicology Letters*, *9*, 45-50.

Yang, G. Y., & Shamsuddin, A. M. (1995). IP6-induced growth inhibition and differentiation of HT-29 human colon cancer cells: involvement of intracellular inositol phosphates. *Anticancer Research*, *15*, 2479-2487.

Yoon, M. J., Kim, E. H., Kwon, T. K., Park, S. A., & Choi, K. S. (2012). Simultaneous mitochondrial Ca(2+) overload and proteasomal inhibition are responsible for the induction of paraptosis in malignant breast cancer cells. *Cancer Letters*, *324*, 197-209.

York, J. D., Odom, A. R., Murphy, R., Ives, E. B., & Wente, S. R. (1999). A phospholipase C-dependent inositol polyphosphate kinase pathway required for efficient messenger RNA export. *Science*, *285*, 96-100.

Young, S. P., & Garner, C. (1990). Delivery of iron to human cells by bovine transferrin. Implications for the growth of human cells in vitro. *Biochemical Journal*, *265*, 587-591.

Zupanska, A., Dziembowska, M., Ellert-Miklaszewska, A., Gaweda-Walerych, K., & Kaminska, B. (2005). Cyclosporine a induces growth arrest or programmed cell death of human glioma cells. *Neurochemistry International*, *47*, 430-441.

APPENDIX A

Development of a *myo*-inositol phosphate liposomal delivery system

Introduction

This appendix describes a portion of work completed during my project not included in the formal section of my thesis. It is included here to provide a record of the work that was completed, and to aid students in the development of similar protocols in the future. This appendix will briefly introduce liposomes, their common methods of production, and our reasons for attempting to develop a liposomal delivery system for IPs. It will then chronologically outline the advancements we made in developing a protocol for liposome production.

Liposomes are artificial, spherical lipid vesicles consisting of one or more lipid bilayers. Their spherical shape results in a liquid comportment capable of packing diverse materials. Use of liposomes as vehicles to transport polar molecules, normally unable to cross the plasma membrane, into cells has become commonplace in the literature. Liposomes are categorized according to the size of their diameter. For example, giant unilamellar vesicles (GUVs) are >1 μm, large unilamellar vesicles (LUVs) are between 1000 – 200 nm, and small unilamellar vesicles (SUVs) are between 200 – 20 nm. Lamellarity refers to the number of lipid bilayers present in a single liposome. In general, SUVs are the most utilized size of liposome for delivery of polar molecules into cells.

Liposomes are easily produced without the use of sophisticated equipment. Certain methods of production such as ethanol injection require the use of sophisticated equipment and are utilized by labs specializing in liposome development. However, the most common technique for producing liposomes in the literature is the Thin Film Hydration (TFH)

method, followed by homogenization steps. This method has become popular on account of its simplicity and its customizability to specific projects. We utilized the TFH method in our protocol development. The key steps in the TFH method are the selection of lipids, formation of a thin lipid film, rehydration and loading, size homogenization of the liposome population, and subsequent removal of nonencapsulated material.

The reason we chose to pursue the development of liposomes capable of delivering IPs to cells was to better investigate their potential effects on human cancer cells. While certain reports indicate $InsP_6$ and several $InsP_5$ isomers may be able to enter cells via endocytosis, IPs are generally considered unable to enter cells on account of their high negative charge. This was a major barrier preventing us from testing the potential intracellular effect our unique, enzymatically derived IPs may have on human cancer cells. Therefore, we embarked on this project with the goal to develop liposomes capable of transporting various novel IPs into human cancer cells.

Generation of SUVs

We based our initial protocol off Gu and colleagues who had already developed a protocol for loading *myo*-inositol pyrophosphates into liposomes and subsequently delivering them to human cells in vitro (Gu et al., 2017). Briefly, L-α-phosphatidycholine (PC) (Sigma; P5394) and cholesterol (ThermoFisher; C-314) were dissolved in chloroform in a 5:1 wt:wt ratio, respectively, in 100 mL round bottom flask (RBFs). The ratio of total lipid mass to chloroform was below 10 mg/mL for all experiments and total chloroform volume never exceeded 8 mL for an individual batch. The chloroform was removed by rotary evaporation under vacuum resulting in a “thin film” of lipids on the surface of the RBF. This lipid film was rehydrated with dH_2O (or specific rehydration buffers) resulting

in the formation of liposomes. At this point, the distribution of liposomes we produced was heterogenous in diameter, with a large fraction being giant liposomes. The next step in liposome production is to reduce the size of the giant liposomes produced to form a homogenous population.

In their protocol, Gu and colleagues extruded their liposomes through 0.2 μm filters resulting in a homogenous distribution of liposomes with a diameter of < 200 nm. This last extrusion step is crucial for obtaining ideal SUVs. Lacking an extruder, we initially omitted this step. Representative images of the liposomes we produced by omitting extrusion are shown in Figure A.1.

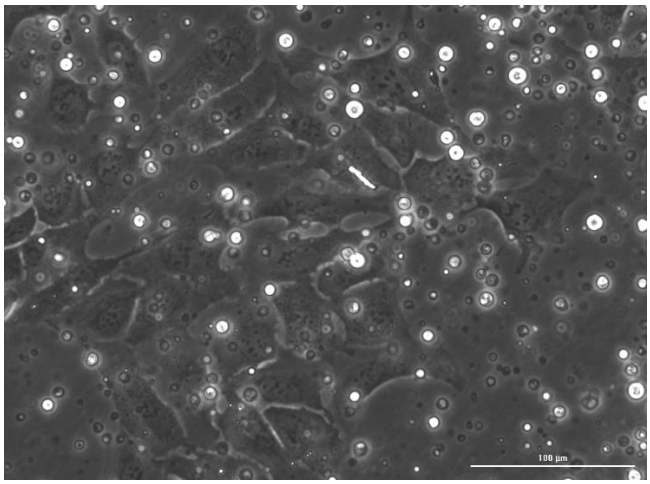

Figure A.1 Giant liposomes on U2-OS cells. Scale bar = 100 μm.

To obtain SUVs we attempted using sonication as an alternative to extrusion. Sonication is an older alternative to extrusion that can disrupt liposome membranes, forcing liposomes to reform as smaller vesicles. We ran trials with both probe and bath sonicators and observed that we could indeed reduce the size of giant liposomes. However, up until this point we had used light microscopy to verify the formation of liposomes. The limit of resolution for light microscopy is 200 nm. Thus, by sonicating our liposomes we lost the

ability to verify their size. The size distribution of a population of liposomes can be assessed by techniques such as dynamic light scattering (DLS) and transmission electron microscopy (TEM). Rather than pursuing these techniques, we decided to purchase an extruder. We recognized in the literature, that it is commonplace to assume a homogenous distribution of SUVs following extrusion. Thus, extrusion provided us with a homogenous population of SUVs, not needing confirmation of its size.

Verification of liposome uptake by cells

A crucial step in developing a liposomal delivery system is verifying that the contents of liposomes are internalized by the target cells. Fluorescent dyes, specifically carboxyfluorescein (FAM), are commonly used to verify liposomal uptake. Packaging a fluorophore such as FAM into liposomes and tracking its uptake by cells confirms liposomal uptake. We prepared FAM loaded liposomes as described above (lacking extrusion), rehydrating the thin film in a PBS buffered 100 mM FAM solution, pH 7. To remove nonencapsulated FAM, the liposome solution was centrifuged at 13000 rcf for 2 minutes and resuspended in PBS. This process was repeated 6 times and images were taken of FAM loaded liposomes (Figure A.2). Green fluorescence in the spherical shapes indicates FAM loading of liposomes.

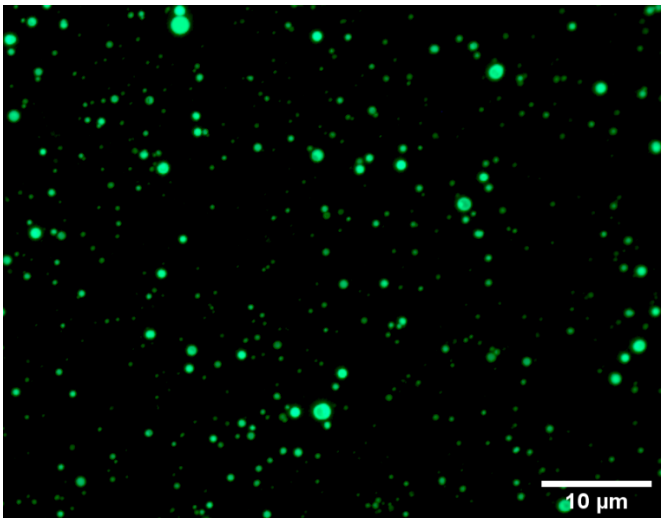

Figure A.2 Carboxyfluorescein loaded liposomes. Scale bar = 10 µm.

Having established that we were able to produce FAM loaded liposomes, we next attempted to verify liposomal uptake by tracking FAM fluorescence in cells. The final optimized protocol we used is described here.

Final optimized protocol

Liposomes were produced by dissolving 15 mg of PC and 3 mg of cholesterol in 2 mL of chloroform in a clean, dry 100 mL RBF. The chloroform was removed by rotary evaporation under vacuum in a hot water bath. The thin film was rehydrated for 25 min with 2 mL of 100 mM FAM, 10 mM HEPES, 100 mM NH_4HCO_3, in dH_2O. The RBF was spun in the hot water bath during the 25 minutes to let the entire surface area of the thin film be rehydrated. The rehydrated solution was extruded for 11 passes through a 0.1 µm filter using an Avanti Polar Lipids Mini-extruder in 900 mL aliquots. An aliquot of 750 µL extruded liposomes was centrifuged for 1 h at 21000 rcf in 4°C and resuspended in 750 µL of dH_2O. The centrifugation and resuspension were repeated twice more. U2-OS cells were treated with 40 µL liposomes per 1 mL media in 12 well plates. Cells were imaged 3 hours

post treatment with liposomes (Figure A.4). The internalization of fluorescence in these cells suggests FAM is being taken up via liposomes.

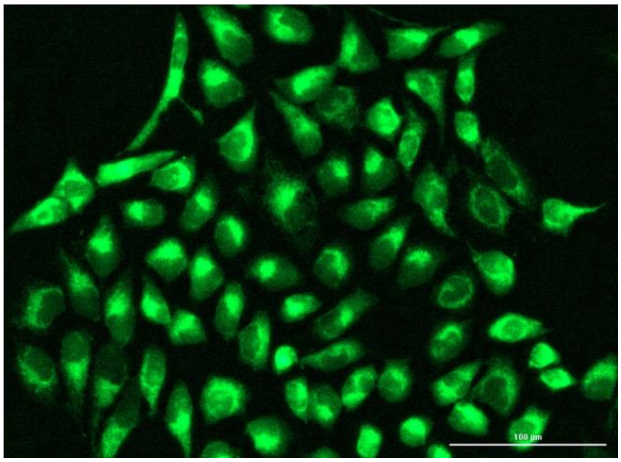

Figure A.3 U2-OS cells treated 40 µL of 100 mM FAM liposomes. Cells were imaged 3 hours post treatment by fluorescent microscopy. Scale bar = 100 µm.

APPENDIX B

Supplementary material

Supplemental Figure B.1

MDD-HPIC Chromatogram of enzymatically derived Ins(1,2,3,4)P_4

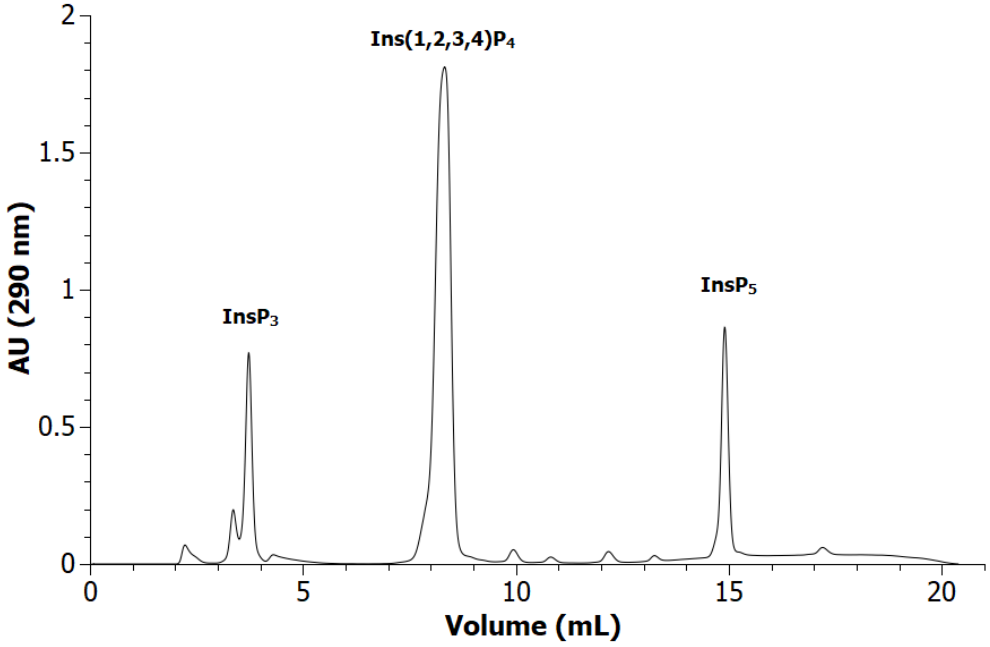

Supplemental Figure B.2

MDD-HPIC Chromatogram of enzymatically derived Ins(2,3,4,5,6)P_5

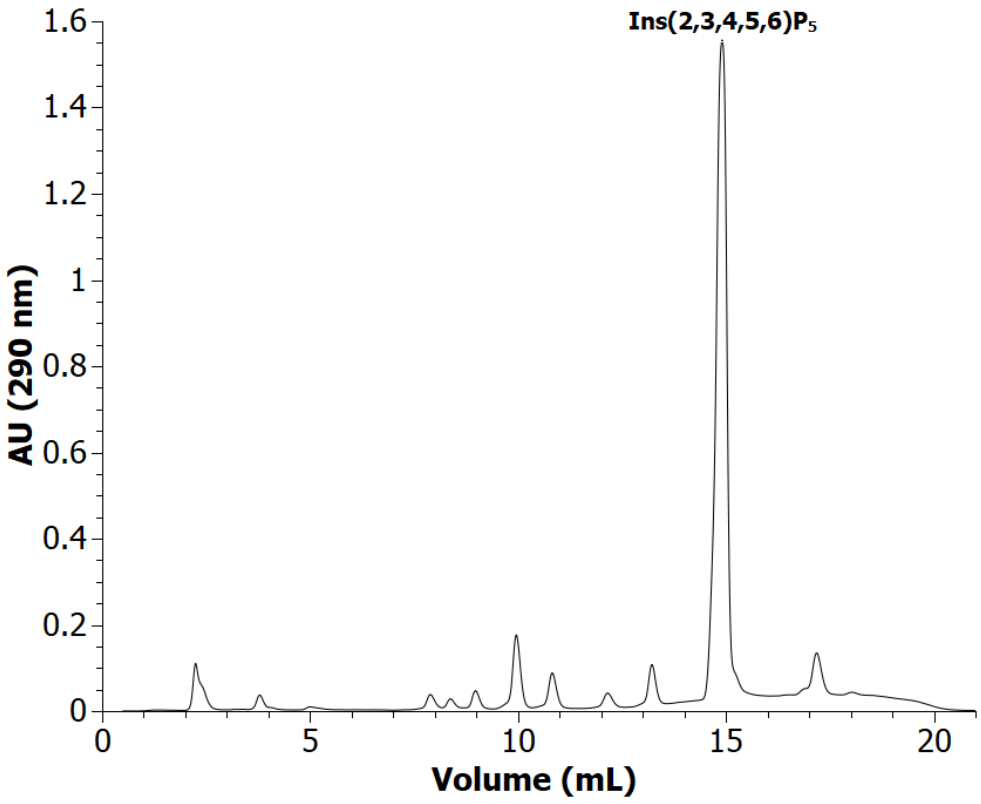

Supplemental Figure B.3

MDD-HPIC Chromatogram of enzymatically derived Ins(1,2,4,5,6)P_5